

Long-baseline neutrino oscillation experiments and CP violation in the lepton sector

S.M. Bilenky

*Joint Institute for Nuclear Research, Dubna, Russia, and
INFN, Sezione di Torino, and Dipartimento di Fisica Teorica, Università di Torino,
Via P. Giuria 1, I-10125 Torino, Italy*

C. Giunti

*INFN, Sezione di Torino, and Dipartimento di Fisica Teorica, Università di Torino,
Via P. Giuria 1, I-10125 Torino, Italy*

W. Grimus

*Institute for Theoretical Physics, University of Vienna,
Boltzmannngasse 5, A-1090 Vienna, Austria
(December 29, 1997)*

Abstract

We discuss possibilities to investigate the effects of CP (and T) violation in the lepton sector in neutrino oscillation experiments. We consider the effects of CP violation in the framework of two schemes of mixing of four massive neutrinos that can accommodate the results of all neutrino oscillation experiments. Using the constraints on the mixing parameters that follow from the results of short-baseline neutrino oscillation experiments, we derive rather strong upper bounds on the effects of CP violation in $\bar{\nu}_\mu \leftrightarrow \bar{\nu}_e$ transitions in long-baseline neutrino oscillation experiments. We show that the effects of CP violation in $\bar{\nu}_\mu \leftrightarrow \bar{\nu}_\tau$ transitions in long-baseline oscillation experiments can be as large as is allowed by the unitarity of the mixing matrix. The matter effects, which complicate the problem of searching for CP violation in long-baseline experiments, are discussed in detail. We consider the T-odd asymmetries whose measurement could allow to reveal T and CP violation in the lepton sector independently from matter effects.

14.60.Pq, 14.60.St

Typeset using REVTeX

I. INTRODUCTION

The violation of CP invariance is one of the most important problems in particle physics. So far, CP violation has only been observed in the $K^0\bar{K}^0$ system [1]. Many future experiments will investigate the effects of CP violation in decays of B mesons and are aimed to reveal the origin of CP violation in the quark sector (for recent reviews see, e.g., Ref. [2]). In the Standard Model of electroweak interactions CP violation resides in a phase in the Cabibbo–Kobayashi–Maskawa mixing matrix [3]. In the lepton sector an analogous mixing matrix is expected to exist if neutrinos are massive and, consequently, it is plausible to assume the presence of CP-violating phases in the neutrino mixing matrix as well.

At present there are some indications that neutrinos are massive and mixed particles coming from the results of solar neutrino experiments (Homestake [4], Kamiokande [5], GALLEX [6], SAGE [7] and Super-Kamiokande [8]), of atmospheric neutrino experiments (Kamiokande [9], IMB [10], Soudan [11] and Super-Kamiokande [12]) and of the accelerator LSND experiment [13]. The analysis of the data of these experiments in terms of neutrino oscillations indicate the existence of three different scales of neutrino mass-squared differences:

$$\Delta m_{\text{sun}}^2 \sim 10^{-5} \text{ eV}^2 \text{ [14]} \quad \text{or} \quad \Delta m_{\text{sun}}^2 \sim 10^{-10} \text{ eV}^2 \text{ [15]}, \quad (1.1)$$

$$\Delta m_{\text{atm}}^2 \simeq 5 \times 10^{-3} \text{ eV}^2 \text{ [12]}, \quad (1.2)$$

$$0.3 \lesssim \Delta m_{\text{LSND}}^2 \lesssim 2.2 \text{ eV}^2 \text{ [13]}. \quad (1.3)$$

The two possibilities for Δm_{sun}^2 correspond, respectively, to the MSW [16] and to the vacuum oscillation (see Refs. [17–19]) solutions of the solar neutrino problem. At present there is no information on CP violation in the lepton sector.

Here we consider possibilities to reveal effects of CP violation in neutrino oscillations in schemes of neutrino mixing that can provide three independent neutrino mass-squared differences. These schemes are based on the assumption that the flavour neutrino fields are superpositions of four massive neutrino fields. This means that the neutrino mixing matrix can contain CP-violating phases and effects of CP violation in the lepton sector could be observed in neutrino oscillation experiments.

In principle, short-baseline (SBL) accelerator neutrino oscillation experiments could be important sources of information on CP-violation in the lepton sector, but in the case of four massive neutrinos only the largest mass-squared difference $\Delta m^2 \equiv \Delta m_{\text{LSND}}^2$ is relevant for SBL oscillations and the effects of CP violation cannot be revealed in SBL experiments [20]. This fact is discussed in Section II, where we review some general aspects of CP violation in neutrino oscillations. In the rest of the paper we discuss the effects of CP violation that can be expected in future accelerator long-baseline (LBL) neutrino oscillation experiments (K2K [21], MINOS [22], ICARUS [23] and others [24]).

In Refs. [25,26] we have shown that among all the possible schemes with four massive neutrinos only two can accommodate the results of all neutrino oscillation experiments (see also Ref. [27]). These two schemes are presented in Section III. In Section IV we apply to these schemes the general methods presented in the Appendices A–C that allow to obtain limits on the parameters that characterize the CP-odd asymmetries in different LBL channels from the exclusion plots obtained in SBL experiments. We show that in the schemes under

consideration there are rather severe constraints on the parameter $I_{e\mu}$ that characterizes CP violations in the $\bar{\nu}_\mu \leftrightarrow \bar{\nu}_e$ channels in vacuum, whereas the parameter $I_{\mu\tau}$ that characterizes CP violations in $\bar{\nu}_\mu \leftrightarrow \bar{\nu}_\tau$ LBL transitions in vacuum can reach its maximum value determined by the unitarity of the mixing matrix.

The possible effects of CP violation in LBL neutrino oscillation experiments have been discussed recently in the literature [28–30] in the framework of three-neutrino schemes that could accommodate the results of some, but not all, neutrino oscillation experiments (in particular, in these schemes the solar neutrino problem cannot be explained with neutrino oscillations). In Section V we apply the methods presented in this paper in order to obtain the limits on the parameters that characterize the CP-odd asymmetries in different LBL channels in the framework of these schemes of mixing of three massive neutrinos.

In Section VI we discuss the implications of matter effects for the possibility to observe CP violation in LBL experiments. Matter effects can be large and they represent a serious problem for the investigation of CP violation in LBL experiments because the interaction of neutrinos and antineutrinos with matter is not CP-symmetric. In order to extract the CP-violating phases of the mixing matrix from the measured asymmetries it is necessary to have detailed information on the absolute values of the elements of the mixing matrix and on the neutrino mass-squared differences. To avoid this problem, we consider the T-odd asymmetries whose measurement could reveal CP violation in the lepton sector independently from the presence of matter (the matter contribution to the effective Hamiltonian is T-symmetric) [31]. Measurements of such asymmetries may be possible in the future, for example, with neutrino beams from muon colliders [32,33].

II. NEUTRINO OSCILLATIONS AND CP VIOLATION

In accordance with the neutrino mixing hypothesis (see, for example, Refs. [17–19]), a left-handed neutrino field $\nu_{\alpha L}$ is a mixture of the left-handed components ν_{kL} of the (Dirac or Majorana) fields of neutrinos with definite masses m_k :

$$\nu_{\alpha L} = \sum_k U_{\alpha k} \nu_{kL} \quad \text{with} \quad \alpha = e, \mu, \tau, s, \dots, \quad (2.1)$$

where U is the unitary mixing matrix. Here $k \geq 3$ and ν_{sL}, \dots are possible sterile neutrino fields. The mixing in Eq.(2.1) implies that the transition probabilities in vacuum of neutrinos and antineutrinos with momentum p at a distance L of the neutrino detector from the neutrino source are given by

$$P_{\nu_\alpha \rightarrow \nu_\beta} = \left| \sum_k U_{\beta k} U_{\alpha k}^* \exp\left(-i \frac{\Delta m_{k1}^2 L}{2p}\right) \right|^2, \quad (2.2)$$

$$P_{\bar{\nu}_\alpha \rightarrow \bar{\nu}_\beta} = \left| \sum_k U_{\beta k}^* U_{\alpha k} \exp\left(-i \frac{\Delta m_{k1}^2 L}{2p}\right) \right|^2, \quad (2.3)$$

where $\Delta m_{k1}^2 \equiv m_k^2 - m_1^2$ (we take $m_1 \leq m_2 \leq \dots$). From Eqs.(2.2) and (2.3) it follows that the transition probabilities of neutrinos and antineutrinos are connected by the relation

$$P_{\nu_\alpha \rightarrow \nu_\beta} = P_{\bar{\nu}_\beta \rightarrow \bar{\nu}_\alpha}. \quad (2.4)$$

This relation reflects CPT invariance.

If CP invariance in the lepton sector holds, then there are conventions for the arbitrary phases such that in the case of Dirac neutrinos we have

$$U_{\alpha k} = U_{\alpha k}^*, \quad (2.5)$$

whereas in the case of Majorana neutrinos we have

$$U_{\alpha k} = -U_{\alpha k}^* \eta_k, \quad (2.6)$$

where $\eta_k = \pm i$ is the CP parity¹ of the Majorana neutrino with mass m_k (see, for example, Ref. [18]). It is obvious that the CP parities η_k do not enter in the expressions for the transitions amplitudes. Hence, in both the Dirac and Majorana cases, CP invariance implies that [35]

$$P_{\nu_\alpha \rightarrow \nu_\beta} = P_{\bar{\nu}_\alpha \rightarrow \bar{\nu}_\beta}. \quad (2.7)$$

Let us introduce the CP-odd asymmetries

$$D_{\alpha;\beta} \equiv P_{\nu_\alpha \rightarrow \nu_\beta} - P_{\bar{\nu}_\alpha \rightarrow \bar{\nu}_\beta}. \quad (2.8)$$

From CPT invariance it follows that

$$D_{\alpha;\beta} = -D_{\beta;\alpha}. \quad (2.9)$$

Furthermore, from the unitarity of the mixing matrix we have

$$\sum_{\beta \neq \alpha} D_{\alpha;\beta} = 0. \quad (2.10)$$

We observe that in the case of transitions among three flavour states (ν_e, ν_μ, ν_τ) the CP asymmetries satisfy the relations [20]

$$D_{e;\mu} = D_{\mu;\tau} = D_{\tau;e}, \quad (2.11)$$

which follow from Eqs.(2.9) and (2.10).

In the general case of mixing of an arbitrary number of massive neutrinos, the transition probabilities are given by

$$P_{\nu_\alpha \rightarrow \nu_\beta}^{(-)} = \sum_j |U_{\alpha j}|^2 |U_{\beta j}|^2 + 2 \sum_{k>j} \text{Re}[U_{\alpha j} U_{\beta j}^* U_{\alpha k}^* U_{\beta k}] \cos \frac{\Delta m_{kj}^2 L}{2p} \pm \frac{1}{2} D_{\alpha;\beta}, \quad (2.12)$$

¹ The CP parities of Majorana neutrinos could be important for neutrinoless double beta-decay; for example, if the ν_k 's have different CP parities, their contributions to the amplitude of neutrinoless double-beta decay could cancel each other [34].

where the plus (minus) sign applies to neutrinos (antineutrinos). The expression for the asymmetries is

$$D_{\alpha;\beta} = \sum_{k>j} I_{\alpha\beta;jk} \sin \frac{\Delta m_{kj}^2 L}{2p}, \quad (2.13)$$

with

$$I_{\alpha\beta;jk} \equiv 4 \operatorname{Im} [U_{\alpha j} U_{\beta j}^* U_{\alpha k}^* U_{\beta k}] . \quad (2.14)$$

These parameters are invariant under rephasing of the neutrino mixing matrix and (apart for a factor 4) are the analogues in the lepton sector of the well-known rephasing-invariant parameters in the quark sector [36–38]. In Sections IV–VI we will derive the constraints on the parameters $I_{\alpha\beta;jk}$ which follow from the results of neutrino oscillation experiments in the framework of schemes with four and three massive neutrinos.

CP violation in the lepton sector can be observed in neutrino oscillation experiments only if at least one of the terms of the sum in Eq.(2.13) does not vanish because of the averaging over the neutrino energy spectrum and the size of the neutrino source and detector.

If only one mass-squared difference (denoted by Δm^2) is relevant for short-baseline neutrino oscillations, the neutrinos can be divided in two groups ν_1, \dots, ν_r and ν_{r+1}, \dots, ν_n with masses $m_1 \leq \dots \leq m_r$ and $m_{r+1} \leq \dots \leq m_n$, respectively, such that in SBL experiments

$$\frac{\Delta m_{kj}^2 L}{2p} \ll 1 \quad \text{for } j, k \leq r \quad \text{or } j, k > r, \quad (2.15)$$

whereas

$$\Delta m_{kj}^2 \simeq \Delta m^2 \quad \text{for } k > r \text{ and } j \leq r. \quad (2.16)$$

In this case, for the CP asymmetries in SBL neutrino oscillation experiments we obtain [20]

$$D_{\alpha;\beta}^{(\text{SBL})} = \left(\sum_{r \geq k > j} + \sum_{k > j > r} + \sum_{k > r \geq j} \right) I_{\alpha\beta;jk} \sin \frac{\Delta m_{kj}^2 L}{2p} \simeq \sum_{k > r \geq j} I_{\alpha\beta;jk} \sin \frac{\Delta m^2 L}{2p} = 0. \quad (2.17)$$

The last step follows from the definition (2.14) and the unitarity of the mixing matrix. Consequently, it is necessary to consider neutrino oscillations in LBL experiments in order to have some possibility to observe effects of CP violation in the lepton sector.

In the rest of this paper we will consider schemes with four and three massive neutrinos, in which only the largest mass-squared difference Δm^2 is relevant for neutrino oscillations in SBL experiments, having a value in the wide range

$$10^{-1} \text{ eV}^2 \leq \Delta m^2 \leq 10^3 \text{ eV}^2, \quad (2.18)$$

which include the interval (1.3) allowed by the results of the LSND experiment.

III. FOUR MASSIVE NEUTRINOS

All existing indications in favour of neutrino oscillations can be accommodated by a scheme with mixing of four massive neutrinos [39,40,25–27]. In Refs. [25,26] we have shown that from the six possible spectral schemes of four massive neutrinos, which correspond to three different scales of mass-squared differences Δm_{kj}^2 , only two schemes are compatible with the results of all experiments (see also Ref. [27]). In these two schemes the four neutrino masses are divided in two pairs of close masses separated by a gap of ~ 1 eV:

$$(A) \quad \underbrace{m_1 < m_2}_{\text{atm}} \ll \underbrace{m_3 < m_4}_{\text{solar}} \quad \text{and} \quad (B) \quad \underbrace{m_1 < m_2}_{\text{solar}} \ll \underbrace{m_3 < m_4}_{\text{atm}}. \quad (3.1)$$

LSND LSND

In scheme A, Δm_{21}^2 is relevant for the explanation of the atmospheric neutrino anomaly and Δm_{43}^2 is relevant for the suppression of solar ν_e 's. In scheme B, the roles of Δm_{21}^2 and Δm_{43}^2 are reversed.

Let us define the quantities c_α (with $\alpha = e, \mu, \tau, s$) as

$$c_\alpha \equiv \sum_{k=1,2} |U_{\alpha k}|^2. \quad (3.2)$$

Taking into account the results of SBL neutrino oscillation experiments and those of solar and atmospheric neutrino experiments, in the two schemes A and B the parameters c_e and c_μ are constrained by [25,26]

$$(A) \quad c_e \leq a_e^0, \quad c_\mu \geq 1 - a_\mu^0, \quad (3.3)$$

$$(B) \quad c_e \geq 1 - a_e^0, \quad c_\mu \leq a_\mu^0, \quad (3.4)$$

where

$$a_\alpha^0 = \frac{1}{2} \left(1 - \sqrt{1 - B_{\alpha;\alpha}^0} \right) \quad (\alpha = e, \mu) \quad (3.5)$$

and $B_{\alpha;\alpha}^0$ is the experimental upper bound for the oscillation amplitude [26]

$$B_{\alpha;\alpha} = 4 c_\alpha (1 - c_\alpha) \quad (3.6)$$

in SBL disappearance experiments. The values of a_e^0 and a_μ^0 obtained, respectively, from the 90% exclusion plots of the Bugey [41] $\bar{\nu}_e \rightarrow \bar{\nu}_e$ reactor experiment and of the CDHS [42] and CCFR [43] $\nu_\mu \rightarrow \nu_\mu$ accelerator experiments are given in Fig. 1 of Ref. [44]. From that figure one can see that a_e^0 is small ($a_e^0 \lesssim 4 \times 10^{-2}$) for Δm^2 in the wide range (2.18) and a_μ^0 is small ($a_\mu^0 \lesssim 10^{-1}$) for $\Delta m^2 \gtrsim 0.5 \text{ eV}^2$. In the following we will use also the upper bounds $A_{\alpha;\beta}^0$ for $\alpha = \mu$ and $\beta = e, \tau$ on the SBL oscillation amplitudes [26]

$$A_{\alpha;\beta} = 4 \left| \sum_{k=1,2} U_{\beta k} U_{\alpha k}^* \right|^2 = 4 \left| \sum_{k=3,4} U_{\beta k} U_{\alpha k}^* \right|^2, \quad (3.7)$$

which are obtained from 90% CL exclusion plots of the BNL E734 [45], BNL E776 [46] and CCFR [47] $\bar{\nu}_\mu \rightarrow \bar{\nu}_e^{(-)}$ appearance experiments and of the FNAL E531 [48] and CCFR [49] $\bar{\nu}_\mu \rightarrow \bar{\nu}_\tau^{(-)}$ appearance experiments. The result of the LSND [13] $\bar{\nu}_\mu \rightarrow \bar{\nu}_e$ appearance experiment, which is crucial for the arguments in favour of the 4-neutrino schemes A and B [25–27], will be of importance in the further discussion mainly through the allowed range (1.3) of Δm^2 .

It can be seen from the neutrino mass spectra (3.1) that the expressions of the oscillation probabilities in scheme B follow from the corresponding expressions in scheme A through the exchange of indices

$$1, 2 \Leftrightarrow 3, 4. \quad (3.8)$$

Since this permutation of indices transforms the conditions (3.3) into $1 - c_e \leq a_e^0$ and $1 - c_\mu \geq 1 - a_\mu^0$, which are identical with those of Eq.(3.4), it follows that the schemes A and B are indistinguishable with neutrino oscillations [50]. Note, however, that these schemes could in principle be distinguished, for instance, in $(\beta\beta)_{0\nu}$ decay or with the measurement of the high-energy part of the β -spectrum of ${}^3\text{H}$ [25,26]. In the following we will perform all calculations in scheme A, but all bounds on CP-violating observables which we will derive hold in both schemes.

Short-baseline neutrino oscillation experiments are sensitive to $\Delta m^2 \equiv \Delta m_{41}^2 \gtrsim 0.1 \text{ eV}^2$ with a distance L between neutrino source and detector such that

$$\frac{\Delta m_{21}^2 L}{2p} \ll 1 \quad \text{and} \quad \frac{\Delta m_{43}^2 L}{2p} \ll 1. \quad (3.9)$$

As discussed in the previous section, with these assumptions on the neutrino mass spectrum there are no effects of CP violation in SBL neutrino oscillations. On the other hand, long-baseline neutrino oscillation experiments are planned to be sensitive to the ‘‘atmospheric neutrino range’’ $10^{-3} \text{ eV}^2 \lesssim \Delta m_{kj}^2 \lesssim 10^{-1} \text{ eV}^2$. In scheme A, the probabilities of $\nu_\alpha \rightarrow \nu_\beta$ and $\bar{\nu}_\alpha \rightarrow \bar{\nu}_\beta$ transitions in LBL experiments are given by

$$P_{\nu_\alpha \rightarrow \nu_\beta}^{(\text{LBL,A})} = \left| U_{\beta 1} U_{\alpha 1}^* + U_{\beta 2} U_{\alpha 2}^* \exp\left(-i \frac{\Delta m_{21}^2 L}{2p}\right) \right|^2 + \left| \sum_{k=3,4} U_{\beta k} U_{\alpha k}^* \right|^2, \quad (3.10)$$

$$P_{\bar{\nu}_\alpha \rightarrow \bar{\nu}_\beta}^{(\text{LBL,A})} = \left| U_{\beta 1}^* U_{\alpha 1} + U_{\beta 2}^* U_{\alpha 2} \exp\left(-i \frac{\Delta m_{21}^2 L}{2p}\right) \right|^2 + \left| \sum_{k=3,4} U_{\beta k}^* U_{\alpha k} \right|^2, \quad (3.11)$$

respectively. Matter effects are not included in these formulas which have been obtained from Eqs.(2.2) and (2.3), respectively, by taking into account that in LBL experiments $\Delta m_{43}^2 L/2p \ll 1$ and averaging out the oscillating terms with phases much larger than 2π ($\Delta m_{kj}^2 L/2p \gg 2\pi$ for $k = 3, 4$ and $j = 1, 2$).

From Eqs.(3.10), (3.11) and (3.8) it follows that the CP-odd asymmetries $D_{\alpha;\beta}^{(\text{LBL})}$ in LBL experiments in the schemes A and B are given by

$$D_{\alpha;\beta}^{(\text{LBL,A})} = I_{\alpha\beta}^{(\text{A})} \sin \frac{\Delta m_{21}^2 L}{2p}, \quad (3.12)$$

$$D_{\alpha;\beta}^{(\text{LBL,B})} = I_{\alpha\beta}^{(\text{B})} \sin \frac{\Delta m_{43}^2 L}{2p}, \quad (3.13)$$

with the oscillation amplitudes (see Eq.(2.14))

$$I_{\alpha\beta}^{(A)} \equiv I_{\alpha\beta;12} \quad \text{and} \quad I_{\alpha\beta}^{(B)} \equiv I_{\alpha\beta;34} . \quad (3.14)$$

In the following we will only study scheme A and drop the superscript A ($I_{\alpha\beta}^{(A)} \equiv I_{\alpha\beta}$) for the reasons mentioned above in the context of Eq.(3.8).

Finally, we want to mention that the phases of the products of elements of the mixing matrix whose imaginary parts give the quantities $I_{e\mu}$, $I_{e\tau}$ and $I_{\mu\tau}$ are not independent [38], as can be seen from the obvious relation

$$\arg [U_{\mu 1} U_{\tau 1}^* U_{\mu 2}^* U_{\tau 2}] = \arg [U_{e 1} U_{\tau 1}^* U_{e 2}^* U_{\tau 2}] - \arg [U_{e 1} U_{\mu 1}^* U_{e 2}^* U_{\mu 2}] , \quad (3.15)$$

which is valid if $I_{e\mu}$, $I_{e\tau}$ and $I_{\mu\tau}$ are all different from zero. Hence, a measurement of $I_{e\mu}$, $I_{e\tau}$ and $I_{\mu\tau}$ can give information on only two independent linear combinations of the three CP-violating phases which are possible in the four-neutrino schemes. In order to obtain information on the values of all the three CP-violating phases it is necessary to measure also some of the other $I_{\alpha\beta;kj}$'s.

IV. CP VIOLATION IN THE SCHEMES WITH FOUR NEUTRINOS

In this section we discuss bounds on the vacuum quantities (3.14). For the reasons explained in Sect. III we confine ourselves to scheme A in the derivations of the bounds. As shown in Appendix B, the unitarity of the mixing matrix implies the ‘‘unitarity bound’’

$$|I_{\alpha\beta}| \leq f(c_\alpha, c_\beta) \quad (4.1)$$

where $f(x, y)$ is the continuous function

$$f(x, y) = \begin{cases} f_1 \equiv xy & \text{for } 2(1-x)(1-y) \geq xy \\ f_2 \equiv 2[(x+y-1)(1-x)(1-y)]^{1/2} & \text{for } 2(1-x)(1-y) < xy \end{cases} \quad (4.2)$$

defined on the unit square $0 \leq x \leq 1$, $0 \leq y \leq 1$. In Fig. 1 we have drawn a contour plot of the function $f(x, y)$, which is helpful for the determination of the maximal allowed value for $f(c_\alpha, c_\beta)$ when c_α and/or c_β are bounded. The dotted line in Fig. 1 is the borderline $g(x) = 2(1-x)/(2-x)$ between the regions where $f = f_1$ and $f = f_2$. Note that f is continuous along this borderline.

In order to determine the maxima of $f(x, y)$, the following considerations are useful (for the details consult Appendix C). Increasing x at fixed y , the function f increases monotonously from $f = 0$ at $x = 0$, until the straight line $y_1(x) = 2 - 2x$ ($1/2 \leq x \leq 1$) depicted in Fig. 1 is reached. There, the value of f is given by $f = y\sqrt{1-y}$. After this intersection, the function f decreases monotonously to $f = 0$ at $x = 1$. From the symmetry $f(x, y) = f(y, x)$, it follows that for fixed x and increasing y the function f increases monotonously from $f = 0$ at $y = 0$ to $f = x\sqrt{1-x}$ when the straight line $y_2(x) = 1 - x/2$ ($0 \leq x \leq 1$) depicted in Fig. 1 is crossed. After this intersection, f decreases monotonously to $f = 0$ at $y = 1$.

The absolute maximum of the function f (see Appendix C) lies at the intersection of the lines y_1 and y_2 and is given by $f_{\max} = 2/3\sqrt{3} \approx 0.385$. Therefore, from the unitarity of the mixing matrix we have an absolute maximum for $|I_{\alpha\beta}|$:

$$|I_{\alpha\beta}| \leq \frac{2}{3\sqrt{3}} \approx 0.385. \quad (4.3)$$

With the help of Fig. 1, one can see that Eq.(4.1) with the constraints (3.3) on c_e and c_μ implies that

$$|I_{e\mu}| \leq \begin{cases} f_2(a_e^0, y_2(a_e^0)) = a_e^0 (1 - a_e^0)^{1/2} & \text{for } a_\mu^0 \geq a_e^0/2, \\ f_2(a_e^0, 1 - a_\mu^0) = 2 [(a_e^0 - a_\mu^0) (1 - a_e^0) a_\mu^0]^{1/2} & \text{for } a_\mu^0 \leq a_e^0/2. \end{cases} \quad (4.4)$$

The solid curve in Fig. 2 shows the limit $|I_{e\mu}| \leq a_e^0 \sqrt{1 - a_e^0}$ with a_e^0 obtained from the 90% CL exclusion plot of the Bugey [41] $\bar{\nu}_e \rightarrow \bar{\nu}_e$ experiment. The dash-dotted curve in Fig. 2 represents the improvement reached with the lower part of Eq.(4.4) at the values of Δm^2 for which $a_\mu^0 \leq a_e^0/2$, with a_μ^0 obtained from the 90% CL exclusion plots of the CDHS [42] and CCFR [43] $\nu_\mu \rightarrow \nu_\mu$ experiments. From this figure one can see that the upper bound for $|I_{e\mu}|$ is very small ($|I_{e\mu}| \lesssim 4 \times 10^{-2}$) for Δm^2 in the wide range (2.18).

The bound represented by the solid curve in Fig. 2 is valid also for $|I_{e\tau}|$, because there is no experimental information on c_τ .

For $|I_{\mu\tau}|$, again by inspection of Fig. 1, one can see that Eq.(4.1) with the constraint (3.3) on c_μ implies that

$$|I_{\mu\tau}| \leq f_2(1 - a_\mu^0, y_2(1 - a_\mu^0)) = (1 - a_\mu^0) \sqrt{a_\mu^0}. \quad (4.5)$$

The solid curve in Fig. 3 represents the corresponding bound obtained from the 90% CL exclusion curves of the CDHS [42] and CCFR [43] $\nu_\mu \rightarrow \nu_\mu$ experiments. For $\Delta m^2 \lesssim 0.3 \text{ eV}^2$ there are no experimental data and therefore $|I_{\mu\tau}|_{\max} \approx 0.385$ by virtue of Eq.(4.3).

Taking into account the expression (3.7) for $A_{\alpha;\beta}$, in both schemes A and B we have also the ‘‘amplitude bound’’ (for the proof of this inequality, see Appendix A)

$$|I_{\alpha\beta}| \leq \frac{1}{2} \sqrt{A_{\alpha;\beta} (4 c_\alpha c_\beta - A_{\alpha;\beta})}. \quad (4.6)$$

With the upper bound $A_{\alpha;\beta} \leq A_{\alpha;\beta}^0$ we obtain

$$|I_{\alpha\beta}| \leq \begin{cases} \frac{1}{2} \sqrt{A_{\alpha;\beta}^0 (4 c_\alpha c_\beta - A_{\alpha;\beta}^0)} & \text{for } A_{\alpha;\beta}^0 \leq 2 c_\alpha c_\beta, \\ c_\alpha c_\beta & \text{for } A_{\alpha;\beta}^0 \geq 2 c_\alpha c_\beta. \end{cases} \quad (4.7)$$

For $|I_{e\mu}|$, with the constraints (3.3), the inequality (4.7) becomes

$$|I_{e\mu}| \leq \begin{cases} \frac{1}{2} \sqrt{A_{\mu;e}^0 (4 a_e^0 - A_{\mu;e}^0)} & \text{for } A_{\mu;e}^0 \leq 2 a_e^0, \\ a_e^0 & \text{for } A_{\mu;e}^0 \geq 2 a_e^0. \end{cases} \quad (4.8)$$

The dashed curve in Fig. 2 shows the limit (4.8) obtained using the 90% exclusion plots of the Bugey [41] $\bar{\nu}_e \rightarrow \bar{\nu}_e$ experiment for the determination of a_e^0 and the BNL E734 [45], BNL E776 [46] and CCFR [47] $\nu_\mu \rightarrow \nu_e$ experiments for the determination of $A_{\mu;e}^0$. One can see that the upper bound for $|I_{e\mu}|$ is extremely small ($|I_{e\mu}| \lesssim 10^{-2}$) for Δm^2 in the wide range (2.18), which includes the LSND-allowed range (1.3).

Since the constraints (3.3) do not put an upper bound on the possible values of c_μ and c_τ , in the case of $|I_{\mu\tau}|$ the inequality (4.7) becomes

$$|I_{\mu\tau}| \leq \frac{1}{2} \sqrt{A_{\mu;\tau}^0 (4 - A_{\mu;\tau}^0)}. \quad (4.9)$$

The dashed curve in Fig. 3 shows the limit (4.9) obtained using the 90% exclusion plots of the FNAL E531 [48] and CCFR [49] $\nu_\mu \rightarrow \nu_\tau$ experiments for the determination of $A_{\mu;\tau}^0$.

The shadowed regions in Figs. 2 and 3 correspond to the range (1.3) of Δm^2 allowed at 90% CL by the results of the LSND and all the other SBL experiments. From Fig. 3 it can be seen that, taking into account the LSND signal, $|I_{\mu\tau}|$ could be close to the maximal value $2/3\sqrt{3}$ allowed by the unitarity of the mixing matrix.

V. THREE MASSIVE NEUTRINOS

Though not all present indications in favour of neutrino mixing can be taken into account in scenarios with mixing of three massive neutrinos, it is nevertheless interesting to investigate also this case with the methods developed in this paper. Let us assume for definiteness that of the two differences of squares of neutrino masses one is relevant for SBL oscillations and the other one for LBL oscillations (see also Refs. [28–30,50]). These assumptions give rise to the following two three-neutrino mass spectra

$$(I) \quad \underbrace{m_1 < m_2}_{\text{SBL}} \ll m_3 \quad \text{and} \quad (II) \quad m_1 \ll \underbrace{m_2 < m_3}_{\text{SBL}}. \quad (5.1)$$

Furthermore, the results of the disappearance experiments allow to define the three regions (see Refs. [51,44,40])

$$\begin{aligned} (1) \quad & |U_{ek}|^2 \geq 1 - a_e^0, & |U_{\mu k}|^2 \leq a_\mu^0, \\ (2) \quad & |U_{ek}|^2 \leq a_e^0, & |U_{\mu k}|^2 \leq a_\mu^0, \\ (3) \quad & |U_{ek}|^2 \leq a_e^0, & |U_{\mu k}|^2 \geq 1 - a_\mu^0, \end{aligned} \quad (5.2)$$

with $k = 3$ for the scheme I and $k = 1$ for the scheme II (for the definition of a_e^0 and a_μ^0 , see Eq.(3.5)). The neutrino and antineutrino LBL oscillation probabilities in scheme I are given by

$$P_{\nu_\alpha \rightarrow \nu_\beta}^{(\text{LBL},I)} = \left| U_{\beta 1} U_{\alpha 1}^* + U_{\beta 2} U_{\alpha 2}^* \exp\left(-i \frac{\Delta m_{21}^2 L}{2p}\right) \right|^2 + |U_{\beta 3}|^2 |U_{\alpha 3}|^2, \quad (5.3)$$

$$P_{\bar{\nu}_\alpha \rightarrow \bar{\nu}_\beta}^{(\text{LBL},I)} = \left| U_{\beta 1}^* U_{\alpha 1} + U_{\beta 2}^* U_{\alpha 2} \exp\left(-i \frac{\Delta m_{21}^2 L}{2p}\right) \right|^2 + |U_{\beta 3}|^2 |U_{\alpha 3}|^2. \quad (5.4)$$

From a comparison of Eqs.(5.3) and (5.4) with Eqs.(3.10) and (3.11), it is obvious that the CP-odd asymmetries $D_{\alpha;\beta}^{(\text{LBL,I})}$ are given by the same formulas (3.12) and (3.14) as in the 4-neutrino case with superscript I instead of A. The transition probabilities in scheme II are obtained from the expressions (5.3) and (5.4) by a cyclic permutation of the indices: $1 \rightarrow 2 \rightarrow 3 \rightarrow 1$. Therefore, as in the case of the schemes A and B for four neutrinos, the bounds on the CP-odd parameters $I_{\alpha\beta}$ are the same in the three neutrino schemes I and II.

The methods for the derivation of the bounds on $I_{\alpha\beta}$ which are described in the appendices for the four-neutrino schemes (3.1) are valid also in the case of mixing of three neutrinos. Obviously, the derivations of the four-neutrino case A (B) are carried over to the three-neutrino case I (II) if we put $U_{\alpha 4} = 0$ ($U_{\alpha 1} = 0$ and change the indices $2, 3, 4 \rightarrow 1, 2, 3$) for all $\alpha = e, \mu, \tau$. This implies that the amplitude bound (A10) applies also to the three neutrino schemes (5.1). In order to derive the unitarity bound from Eq.(A10), one must notice that from the unitarity of the 3×3 mixing matrix we have $A_{\alpha;\beta} = 4(1 - c_\alpha)(1 - c_\beta)$ and $c_\alpha + c_\beta \geq 1$. Hence, the equality sign applies in Eq.(B2) and there is no such distinction as defined by Eq.(B4). Consequently, by simple substitution of $A_{\alpha;\beta} = 4(1 - c_\alpha)(1 - c_\beta)$ in Eq.(A10), in the case of mixing of three neutrinos one obtains the unitarity bound (B6), i.e.

$$|I_{\alpha\beta}| \leq f_2(c_\alpha, c_\beta). \quad (5.5)$$

Notice that $f_2(c_\alpha, c_\beta)$ vanishes on the unitarity boundary $c_\alpha + c_\beta = 1$. Since the maxima of $f(c_\alpha, c_\beta)$ and $f_2(c_\alpha, c_\beta)$ coincide and are reached for $c_\alpha = c_\beta = 2/3$ (see Appendix C), the absolute maximum $|I_{\alpha\beta}|_{\text{max}} = 2/3\sqrt{3}$ of the 4-neutrino case extends its validity to three neutrinos².

Furthermore, since in the 3-neutrino case the CP-odd asymmetries in different oscillation channels are connected by Eq.(2.11), we have

$$I_{e\mu} = I_{\mu\tau} = I_{\tau e}. \quad (5.6)$$

In the following we will give LBL bounds for each of the regions (5.2), along the lines of the previous 4-neutrino section.

Region 1. With respect to SBL and LBL neutrino oscillations, the 3-neutrino schemes I and II in Region 1 correspond to the 4-neutrino schemes A and B, respectively, with the same bounds on $|I_{e\mu}|$ (Eqs.(4.4), (4.8) and Fig. 2). Because of Eq.(5.6) the stringent bounds on $|I_{e\mu}|$ given in Fig. 2 are valid also for $|I_{\mu\tau}|$.

Region 2. Actually, this Region is disfavoured by the results of the LSND experiment (see Refs. [51,44,40,26]). Also the results of the atmospheric neutrino experiments [9–12] taken together with the results of the CHOOZ experiment [52] indicate that this Region is disfavoured. Indeed, in this region c_τ is small ($c_\tau \leq a_e^0 + a_\mu^0$) and the atmospheric neutrino anomaly can be explained only with dominant $\nu_\mu \leftrightarrow \nu_e$ oscillations, which are forbidden by the results of the CHOOZ experiment. Since these evidences could disappear when the

²This value corresponds to the maximal value of the Jarlskog parameter J [36,37] for CP violation in the Kobayashi–Maskawa matrix, $|J|_{\text{max}} = 1/6\sqrt{3}$, with an additional factor 4 due to the definition (2.14).

results of future more accurate experiments will be available, let us discuss the bounds on CP violation with the methods described in the appendices. They are given by the amplitude bound

$$|I_{e\mu}| \leq \frac{1}{2} \sqrt{A_{\mu;e}^0 (4 - A_{\mu;e}^0)} \quad (5.7)$$

and the unitarity bound

$$|I_{e\mu}| \leq f_2(1 - a_e^0, 1 - a_\mu^0) = 2 \sqrt{a_e^0 a_\mu^0 (1 - a_e^0 - a_\mu^0)}. \quad (5.8)$$

Both bounds are less restrictive than the corresponding bounds in Region 1. By Eq.(5.6) these bounds hold in all neutrino transition channels.

Region 3. In this region, where $c_e \geq 1 - a_e^0$ and $c_\mu \leq a_\mu^0$, the full set of atmospheric neutrino data cannot be explained in the framework discussed here [26]. Applying nevertheless our methods for obtaining bounds on CP violation, we get the results

$$|I_{e\mu}| \leq \frac{1}{2} \sqrt{A_{\mu;e}^0 (4 a_\mu^0 - A_{\mu;e}^0)} \quad (5.9)$$

and

$$|I_{e\mu}| \leq \begin{cases} a_\mu^0 (1 - a_\mu^0)^{1/2} & \text{for } a_e^0 \geq a_\mu^0/2, \\ 2 [(a_\mu^0 - a_e^0) (1 - a_\mu^0) a_e^0]^{1/2} & \text{for } a_e^0 \leq a_\mu^0/2. \end{cases} \quad (5.10)$$

The amplitude bound is more stringent than the one in Region 2, but less restrictive than the one in Region 1 and in the 4-neutrino schemes A and B (for $a_e^0 < a_\mu^0$). From Eq.(5.6) it follows that the bounds (5.9) and (5.10) are valid also for the parameter $|I_{\mu\tau}|$ that characterizes the CP-odd asymmetry in the $\nu_\mu \rightarrow \nu_\tau$ channel.

Summarizing the results of this section, we have shown that in regions 2 and 3 the strong bounds of region 1 and of the 4-neutrino schemes A and B on $|I_{e\mu}|$ are somewhat relaxed. However, regions 2 and 3 are disfavoured by present hints for neutrino oscillations.

Let us also emphasize that the solar neutrino problem cannot be explained by neutrino oscillations in the three-neutrino schemes considered in this section. Hence, we regard them as remote possibilities.

VI. MATTER EFFECTS AND CP VIOLATION

Since in LBL neutrino oscillation experiments the neutrino beam travels a long distance through the earth's crust, matter effects influence the neutrino oscillation probabilities. The effective Hamiltonians in the flavour basis of neutrinos and antineutrinos in the case of mixing of four neutrinos are given, respectively, by³

³Since active and sterile neutrinos are present in the schemes under consideration, both charged-current and neutral-current interactions contribute to the effective Hamiltonians.

$$H_\nu = \frac{1}{2p} \left(U \hat{M}^2 U^\dagger + \text{diag}(a_{CC}, 0, 0, a_{NC}) \right), \quad (6.1)$$

$$H_{\bar{\nu}} = \frac{1}{2p} \left(U^* \hat{M}^2 U^T - \text{diag}(a_{CC}, 0, 0, a_{NC}) \right), \quad (6.2)$$

where a_{CC} and a_{NC} are given by [16]

$$a_{CC} = 2\sqrt{2} G_F N_e p \simeq 2.3 \times 10^{-4} \text{ eV}^2 \left(\frac{\rho}{3 \text{ g cm}^{-3}} \right) \left(\frac{p}{1 \text{ GeV}} \right), \quad (6.3)$$

$$a_{NC} = \sqrt{2} G_F N_n p \simeq \frac{1}{2} a_{CC}, \quad (6.4)$$

respectively, and $\hat{M}^2 = \text{diag}(m_1^2, m_2^2, m_3^2, m_4^2)$. Here G_F is the Fermi constant, N_e and N_n are the electron and neutron number density, respectively, and ρ is the density of matter. With an average density of approximately 3 g cm^{-3} in the lithosphere we get

$$\frac{a_{CC} L}{2p} \simeq 0.58 \times 10^{-3} \left(\frac{L}{1 \text{ km}} \right). \quad (6.5)$$

Therefore, large matter effects are to be expected for baselines $L \gtrsim 1000 \text{ km}$.

In the following we apply the simplifying approximation of constant electron and neutron number densities, which is rather accurate in the case of LBL experiments. In order to obtain the neutrino oscillation probabilities in matter we have to diagonalize the Hamiltonians (6.1) and (6.2) with unitary matrices U' and \bar{U}' , respectively, leading to the eigenvalues $\epsilon_j/2p$ of H_ν and $\bar{\epsilon}_j/2p$ of $H_{\bar{\nu}}$. Thus, we have

$$H_\nu = U' \frac{\hat{\epsilon}}{2p} U'^\dagger \quad \text{and} \quad H_{\bar{\nu}} = \bar{U}'^* \frac{\hat{\bar{\epsilon}}}{2p} \bar{U}'^T \quad (6.6)$$

with the diagonal matrices $\hat{\epsilon} = \text{diag}(\epsilon_1, \epsilon_2, \epsilon_3, \epsilon_4)$ and $\hat{\bar{\epsilon}} = \text{diag}(\bar{\epsilon}_1, \bar{\epsilon}_2, \bar{\epsilon}_3, \bar{\epsilon}_4)$ for neutrinos and antineutrinos, respectively (in the limit $a_{CC}, a_{NC} \rightarrow 0$ of vanishing matter effects we get $U', \bar{U}' \rightarrow U$ and $\epsilon_j, \bar{\epsilon}_j \rightarrow m_j^2$).

Analogously to the definition of $I_{\alpha\beta;jk}$ in Eq.(2.14), it is useful to define

$$I'_{\alpha\beta;jk} \equiv 4 \text{Im} [U'_{\alpha j} U'^*_{\beta j} U'^*_{\alpha k} U'_{\beta k}] \quad \text{and} \quad \bar{I}'_{\alpha\beta;jk} \equiv 4 \text{Im} [\bar{U}'_{\alpha j} \bar{U}'^*_{\beta j} \bar{U}'^*_{\alpha k} \bar{U}'_{\beta k}]. \quad (6.7)$$

The usefulness of these definitions lies in the fact that *for the proof of the existence of CP violation due to neutrino mixing the quantities $I'_{\alpha\beta;jk}$ and $\bar{I}'_{\alpha\beta;jk}$ are as good as $I_{\alpha\beta;jk}$* . In other words, $I_{\alpha\beta;jk} = 0$ for all values of the indices α, β, j, k if and only if $I'_{\alpha'\beta';j'k'} = 0$ ($\bar{I}'_{\alpha'\beta';j'k'} = 0$) for all values of α', β', j', k' . Let us prove this statement for $I'_{\alpha\beta;jk}$ (an analogous proof holds in the case of $\bar{I}'_{\alpha\beta;jk}$). First we assume that $I_{\alpha\beta;jk} = 0$ for all values of α, β, j, k . This is possible only if the mixing matrix U can be written as $U = e^{i\rho} \tilde{U} e^{i\sigma}$, where ρ and σ are real diagonal matrices and \tilde{U} is real. Since the matter part in the Hamiltonian (6.1) is real and diagonal, the effective Hamiltonian (6.1) can be written as

$$H_\nu = e^{i\rho} \frac{1}{2p} \left(\tilde{U} \hat{M}^2 \tilde{U}^\dagger + \text{diag}(a_{CC}, 0, 0, a_{NC}) \right) e^{-i\rho} \equiv e^{i\rho} \tilde{H}_\nu e^{-i\rho}, \quad (6.8)$$

where \tilde{H}_ν is a real and symmetric matrix. Hence, the matrix U' can be written as $U' = e^{i\rho}\tilde{U}'$ where \tilde{U}' is real. This form of U' implies that $I'_{\alpha\beta;jk} = 0$ for all values of α, β, j, k . In order to prove the inverse statement, i.e. that $I_{\alpha\beta;jk} = 0$ for all values of α, β, j, k if $I'_{\alpha'\beta';j'k'} = 0$ for all values of α', β', j', k' , we note that

$$UM^2U^\dagger = U'\hat{\epsilon}U'^\dagger - \text{diag}(a_{CC}, 0, 0, a_{NC}). \quad (6.9)$$

Now the rôles of U and U' are exchanged. Hence, the same reasoning as before leads to the inverse statement.

The possibility of finding evidence for CP violation in the lepton sector through the quantities $I'_{\alpha\beta;jk}$ and $\bar{I}'_{\alpha\beta;jk}$ leads us to the search for methods that could allow to extract these quantities from the transition probabilities of neutrinos and antineutrinos measured in long-baseline oscillation experiments.

The formula in Eq.(2.12) for the probability of $\nu_\alpha \rightarrow \nu_\beta$ transitions is adapted to the matter case by the substitutions $U \rightarrow U'$ and $I \rightarrow I'$ for neutrinos and $U \rightarrow \bar{U}'$ and $I \rightarrow \bar{I}'$ for antineutrinos:

$$P_{\nu_\alpha \rightarrow \nu_\beta} = \sum_j |U'_{\alpha j}|^2 |U'_{\beta j}|^2 + 2 \sum_{k>j} \text{Re}[U'_{\alpha j} U'_{\beta j}{}^* U'_{\alpha k} U'_{\beta k}{}^*] \cos \frac{\epsilon_{kj} L}{2p} + \frac{1}{2} \sum_{k>j} I'_{\alpha\beta;jk} \sin \frac{\epsilon_{kj} L}{2p}, \quad (6.10)$$

$$P_{\bar{\nu}_\alpha \rightarrow \bar{\nu}_\beta} = \sum_j |\bar{U}'_{\alpha j}|^2 |\bar{U}'_{\beta j}|^2 + 2 \sum_{k>j} \text{Re}[\bar{U}'_{\alpha j} \bar{U}'_{\beta j}{}^* \bar{U}'_{\alpha k} \bar{U}'_{\beta k}{}^*] \cos \frac{\bar{\epsilon}_{kj} L}{2p} - \frac{1}{2} \sum_{k>j} \bar{I}'_{\alpha\beta;jk} \sin \frac{\bar{\epsilon}_{kj} L}{2p}, \quad (6.11)$$

with $\epsilon_{kj} \equiv \epsilon_k - \epsilon_j$ and $\bar{\epsilon}_{kj} \equiv \bar{\epsilon}_k - \bar{\epsilon}_j$. From these two equations it is clear that in matter the transition probabilities of neutrinos and antineutrinos are different even if CP is conserved, i.e. if all the quantities $I'_{\alpha\beta;jk}$ and $\bar{I}'_{\alpha\beta;jk}$ are equal to zero. Hence, simple measurements of the asymmetries (2.8) do not allow to obtain direct information on CP violation [28–30]. This is due to the fact that the matter contribution to the effective neutrino and antineutrino Hamiltonians (6.1), (6.2) is not CP-symmetric. However, since the matter contribution to the effective neutrino (antineutrino) Hamiltonian is real and the matter density is symmetric along the path of the neutrino beam in terrestrial long-baseline experiments, matter effects are T-symmetric [31]. In other words, there is no difference in the matter contributions to the $\nu_\alpha \rightarrow \nu_\beta$ and $\bar{\nu}_\alpha \rightarrow \bar{\nu}_\beta$ channels and a difference of the corresponding transition probabilities can only be due to a fundamental violation of T in the lepton sector. Since the CPT theorem implies that a violation of T is equivalent to a violation of CP, we are lead to explore the possibility to obtain direct evidence of CP and T violation in the lepton sector through measurements of the T-odd asymmetries

$$T_{\alpha\beta} \equiv P_{\nu_\alpha \rightarrow \nu_\beta} - P_{\nu_\beta \rightarrow \nu_\alpha} \quad \text{and} \quad \bar{T}_{\alpha\beta} \equiv P_{\bar{\nu}_\alpha \rightarrow \bar{\nu}_\beta} - P_{\bar{\nu}_\beta \rightarrow \bar{\nu}_\alpha} \quad (6.12)$$

in long-baseline oscillation experiments. In the case of a constant matter density along the neutrino path (which is a good approximation for terrestrial LBL experiments with a baseline shorter than about 4000 km), from Eqs.(6.10) and (6.11) it is straightforward to obtain the following expressions for the T-odd asymmetries:

$$T_{\alpha\beta} = \sum_{k>j} I'_{\alpha\beta;jk} \sin \frac{\epsilon_{kj} L}{2p} \quad \text{and} \quad \bar{T}_{\alpha\beta} = \sum_{k>j} \bar{I}'_{\alpha\beta;jk} \sin \frac{\bar{\epsilon}_{kj} L}{2p}. \quad (6.13)$$

It is clear that finding $T_{\alpha\beta}$ and/or $\bar{T}_{\alpha\beta}$ different from zero would be a direct evidence of T (and CP) violation in the lepton sector independent from matter effects.

The T-odd asymmetries (6.12) cannot be measured in the accelerator LBL experiments of the first generation [21–23] because the initial beam will contain almost exclusively ν_μ . In order to have some possibility to measure the T-odd asymmetries it will be necessary to wait for the second generation of accelerator LBL experiments, as those that will use $\nu_\mu + \bar{\nu}_e$ and $\bar{\nu}_\mu + \nu_e$ neutrino beams from a muon collider [32,33].

Let us now consider the four-neutrino schemes (3.1), whose phenomenology of CP violation in long-baseline neutrino oscillation experiments in vacuum has been discussed in Sections III and IV. We will discuss explicitly only the neutrino T-odd asymmetries $T_{\alpha\beta}$ in the scheme A, but all the conclusions are valid also for the antineutrino T-odd asymmetries $\bar{T}_{\alpha\beta}$ in scheme A and for the neutrino and antineutrino T-odd asymmetries in scheme B (with the exchange of indices given in Eq.(3.8)).

In Ref. [50] we have shown that apart from small corrections of order $a_{CC}/\Delta m^2$, one can decompose U' into

$$U' = UR \quad \text{with} \quad R = \begin{pmatrix} R_{\text{atm}} & 0 \\ 0 & R_{\text{sun}} \end{pmatrix}, \quad (6.14)$$

where R_{atm} and R_{sun} are 2×2 unitary matrices. The block structure of R implies that

$$\sum_{j=1,2} U'_{\alpha j} U'_{\beta j}{}^* = \sum_{j=1,2} U_{\alpha j} U_{\beta j}{}^* \quad (6.15)$$

and therefore

$$c_\alpha \equiv \sum_{j=1,2} |U_{\alpha j}|^2 = \sum_{j=1,2} |U'_{\alpha j}|^2. \quad (6.16)$$

Since the bounds on $I_{\alpha\beta} \equiv I_{\alpha\beta;12}$ derived in Section IV depend only on quantities of the type (6.15) and (6.16), we arrive at the interesting conclusion that the upper bounds on $I_{\alpha\beta}$ are also valid for

$$I'_{\alpha\beta} \equiv I'_{\alpha\beta;12} \quad \text{and} \quad \bar{I}'_{\alpha\beta} \equiv \bar{I}'_{\alpha\beta;12}. \quad (6.17)$$

In this sense the upper bounds represented by the curves in Figs. 2 and 3 include matter effects.

Using a method analogous to that employed for the derivation of Eq.(3.10), for the probability of $\nu_\alpha \rightarrow \nu_\beta$ LBL transitions in matter we obtain

$$\begin{aligned} P_{\nu_\alpha \rightarrow \nu_\beta}^{(\text{LBL})} &= |U'_{\beta 1} U'_{\alpha 1}{}^* + U'_{\beta 2} U'_{\alpha 2}{}^* e^{-i\phi}|^2 + |U'_{\beta 3} U'_{\alpha 3}{}^* + U'_{\beta 4} U'_{\alpha 4}{}^* e^{-i\omega}|^2 \\ &= \sum_k |U'_{\beta k}|^2 |U'_{\alpha k}|^2 + 2 \text{Re}[U'_{\alpha 1} U'_{\beta 1}{}^* U'_{\alpha 2}{}^* U'_{\beta 2}] \cos \phi + 2 \text{Re}[U'_{\alpha 3} U'_{\beta 3}{}^* U'_{\alpha 4}{}^* U'_{\beta 4}] \cos \omega \\ &\quad + \frac{1}{2} I'_{\alpha\beta} \sin \phi + \frac{1}{2} J'_{\alpha\beta} \sin \omega, \end{aligned} \quad (6.18)$$

with the definitions

$$\phi \equiv \frac{\epsilon_2 - \epsilon_1}{2p}L, \quad \omega \equiv \frac{\epsilon_4 - \epsilon_3}{2p}L \quad \text{and} \quad J'_{\alpha\beta} \equiv I'_{\alpha\beta;34}. \quad (6.19)$$

The expressions for the quantities $\epsilon_2 - \epsilon_1$ and $\epsilon_4 - \epsilon_3$ in terms of the neutrino mixing parameters and of the matter density have been derived in Ref. [50].

From Eq.(6.18), for the neutrino T-odd asymmetries we obtain the expression

$$T_{\alpha\beta} = I'_{\alpha\beta} \sin \phi + J'_{\alpha\beta} \sin \omega. \quad (6.20)$$

Therefore, in matter the T-odd asymmetry $T_{\alpha\beta}$ depends not only on the parameter $I'_{\alpha\beta}$ relative to the atmospheric sector (see Eq.(6.14) and the definitions (6.7) and (6.17)), but also on the parameter $J'_{\alpha\beta}$ relative to the solar sector. In Ref. [50] we have shown that in the case of accelerator LBL experiments the maximal value of the parameter ω is given by

$$\omega_{\max} \simeq \frac{3}{2} \frac{a_{CC}L}{2p} = \frac{3}{2} \sqrt{2} G_F N_e L = 8.6 \times 10^{-4} \left(\frac{L}{1\text{km}} \right) \quad (6.21)$$

for $\rho = 3 \text{ g cm}^{-3}$. Notice that the value of ω_{\max} does not depend on the neutrino energy, but only on the propagation distance L . From Eq.(6.21) one can see that the contribution of the term in Eq.(6.20) proportional to $\sin \omega$ could be relevant for $L \gtrsim 100 \text{ km}$ and therefore cannot be neglected in the analysis of the results of LBL experiments.

As we have seen above, the upper bounds on $I_{\alpha\beta} \equiv I_{\alpha\beta;12}$ are also valid for $I'_{\alpha\beta}$ and $\bar{I}'_{\alpha\beta}$. An analogous reasoning leads to the conclusion that the upper bounds on the parameters

$$J_{\alpha\beta} \equiv I_{\alpha\beta;34} \quad (6.22)$$

are also valid for $J'_{\alpha\beta}$ and $\bar{J}'_{\alpha\beta} \equiv \bar{I}'_{\alpha\beta;34}$. Hence we are lead to the investigation of the upper bounds for the parameters $J_{\alpha\beta}$. Following the methods presented in the Appendices A–C, one can derive the unitarity bound

$$|J_{\alpha\beta}| \leq f(1 - c_\alpha, 1 - c_\beta) \quad (6.23)$$

and the amplitude bound

$$|J_{\alpha\beta}| \leq \frac{1}{2} \sqrt{A_{\alpha;\beta} [4(1 - c_\alpha)(1 - c_\beta) - A_{\alpha;\beta}]}. \quad (6.24)$$

Taking into account the constraints (3.3) on c_e and c_μ obtained from the exclusion curves of SBL reactor and accelerator disappearance experiments, the unitarity bound for $|J_{e\mu}|$ is given by

$$|J_{e\mu}| \leq \begin{cases} f_2(a_\mu^0, y_2(a_\mu^0)) = a_\mu^0 (1 - a_\mu^0)^{1/2} & \text{for } a_e^0 \geq a_\mu^0/2, \\ f_2(a_\mu^0, 1 - a_e^0) = 2 [(a_\mu^0 - a_e^0)(1 - a_\mu^0) a_e^0]^{1/2} & \text{for } a_e^0 \leq a_\mu^0/2. \end{cases} \quad (6.25)$$

The numerical value of this bound, obtained from the 90% CL exclusion plot of the Bugey [41] $\bar{\nu}_e \rightarrow \bar{\nu}_e$ experiment and from the 90% CL exclusion plots of the CDHS [42] and CCFR [43] $\nu_\mu \rightarrow \nu_\mu$ experiments, is shown by the solid curve in Fig. 4. The dashed curve in Fig. 4 represents the amplitude bound

$$|J_{e\mu}| \leq \begin{cases} \frac{1}{2} \sqrt{A_{\mu;e}^0 (4a_\mu^0 - A_{\mu;e}^0)} & \text{for } A_{\mu;e}^0 \leq 2a_\mu^0, \\ a_\mu^0 & \text{for } A_{\mu;e}^0 \geq 2a_\mu^0, \end{cases} \quad (6.26)$$

obtained from the 90% CL exclusion plots of the CDHS [42] and CCFR [43] $\nu_\mu \rightarrow \nu_\mu$ experiments and from the 90% CL exclusion plots of the BNL E734 [45], BNL E776 [46] and CCFR [47] $\bar{\nu}_\mu \rightarrow \bar{\nu}_e$ experiments. The shadowed region corresponds to the range (1.3) of Δm^2 allowed at 90% CL by the results of the LSND and all the other SBL experiments. From Fig. 4 it can be seen that $|J_{e\mu}| \lesssim 10^{-1}$ for $\Delta m^2 \gtrsim 0.27 \text{ eV}^2$, which is an interval that includes the LSND-allowed range (1.3).

For $|J_{\mu\tau}|$ we have the unitarity bound

$$|J_{\mu\tau}| \leq f_2(a_\mu^0, y_2(a_\mu^0)) = a_\mu^0 \sqrt{1 - a_\mu^0}. \quad (6.27)$$

This limit is more stringent than the corresponding one for $|I_{\mu\tau}|$ given in Eq.(4.5). Its numerical value obtained from the 90% CL exclusion plots of the CDHS [42] and CCFR [43] $\nu_\mu \rightarrow \nu_\mu$ experiments is shown by the solid curve in Fig. 5. The dashed curve in Fig. 5 represents the value of the amplitude bound

$$|J_{\mu\tau}| \leq \begin{cases} \frac{1}{2} \sqrt{A_{\mu;\tau}^0 (4a_\mu^0 - A_{\mu;\tau}^0)} & \text{for } A_{\mu;\tau}^0 \leq 2a_\mu^0, \\ a_\mu^0 & \text{for } A_{\mu;\tau}^0 \geq 2a_\mu^0, \end{cases} \quad (6.28)$$

obtained from the 90% CL exclusion plots of the CDHS [42] and CCFR [43] $\nu_\mu \rightarrow \nu_\mu$ experiments and from the 90% exclusion plots of the FNAL E531 [48] and CCFR [49] $\nu_\mu \rightarrow \nu_\tau$ experiments. From Fig. 5 one can see that $|J_{\mu\tau}| \lesssim 0.25$ for $\Delta m^2 \gtrsim 0.3 \text{ eV}^2$, including the LSND-allowed range (1.3), and $|J_{\mu\tau}| \lesssim 8 \times 10^{-2}$ for $\Delta m^2 \gtrsim 0.5 \text{ eV}^2$.

Since $1 - c_e$ is large and there is no constraint on the value of c_τ (and the available information on $A_{e;\tau}$ is rather poor), the parameter $|J_{e\tau}|$ is only subject to the unitarity bound

$$|J_{e\tau}| \leq f_2(1 - a_e^0, y_2(1 - a_e^0)) = (1 - a_e^0) \sqrt{a_e^0}. \quad (6.29)$$

This bound is much less stringent than the corresponding one for $|I_{e\tau}|$, represented by the upper function in Eq.(4.4) and depicted as the solid curve in Fig. 2. Since $a_e^0 \lesssim 4 \times 10^{-2}$ for Δm^2 in the wide range (2.18), we obtain the upper bound $|I_{e\tau}| \lesssim 0.2$, which is about half of the unitarity limit $2/3\sqrt{3} \simeq 0.385$.

From the bounds depicted in Figs. 2 and 4, it is clear that the observation of a non-zero T-odd asymmetry $T_{\mu e}$ (and $\bar{T}_{\mu e}$) in future LBL experiments is a very difficult task. On the other hand, from Figs. 3 and 5 one can see that the T-odd asymmetry $T_{\mu\tau}$ (and $\bar{T}_{\mu\tau}$) could be rather large, close to the maximal value allowed by the unitarity of the neutrino mixing matrix. Also the T-odd asymmetry $T_{e\tau}$ (and $\bar{T}_{e\tau}$) could be rather large, but not more than half of the maximal value allowed by the unitarity of the neutrino mixing matrix and only if the matter effect is important and enhances the contribution of $J'_{e\tau}$. Hence, we conclude that long-baseline $\nu_\mu \leftrightarrow \nu_\tau$ (and $\bar{\nu}_\mu \leftrightarrow \bar{\nu}_\tau$) experiments are favoured for the investigation of

CP (and T) violation in the lepton sector if the four-neutrino schemes (3.1) are realized in nature.

We would also like to mention that the CP-odd parameters $J_{\alpha\beta}$ are relevant for the CP-odd asymmetries that could be measured by extremely long-baseline (ELBL) oscillation experiments with neutrino beams propagating in vacuum, for which $\Delta m_{21}^2 L/2p \gg 2\pi$ and $\Delta m_{43}^2 L/2p \sim 1$ (in scheme A),

$$D_{\alpha;\beta}^{(\text{ELBL})} = J_{\alpha\beta} \sin \frac{\Delta m_{43}^2 L}{2p}, \quad (6.30)$$

although we do not know if it will ever be possible to make such experiments.

Concluding this Section, we briefly discuss the matter effects in the case of the 3-neutrino schemes considered in Section V. We consider, for simplicity, only scheme I, but analogous conclusions are valid in scheme II. The 3-neutrino scheme I corresponds to the 4-neutrino scheme A, with the difference that the solar sector of the mixing matrix is absent, i.e. $U_{\alpha 4} = 0$ for $\alpha = e, \mu, \tau$ and $R_{\text{sun}} = 1$ (apart from negligible corrections of order $a_{CC}/\Delta m^2$). Hence, in the 3-neutrino scheme I the neutrino T-odd asymmetries $T_{\alpha\beta}$ (see Eq.(6.12)) are given by Eq.(6.20) with $J'_{\alpha\beta} = 0$. Using the same reasoning as that employed in the case of the 4-neutrino schemes, one can see that the upper bounds on $I_{\alpha\beta}$ derived in Section V in the case of the 3-neutrino schemes are also valid for $I'_{\alpha\beta}$ and $\bar{I}'_{\alpha\beta}$. Hence, $T_{e\mu}$ is very small if the neutrino mixing parameters lie in region 1 and is less suppressed in regions 2 and 3.

VII. CONCLUSIONS

In this paper we have considered possibilities to reveal effects of CP-violation in the lepton sector in future accelerator long-baseline (LBL) experiments (K2K [21], MINOS [22], ICARUS [23] and others [24]).

At present there are three experimental indications in favour of neutrino oscillations which correspond to three different scales of neutrino mass-squared differences: the solar neutrino deficit, the atmospheric neutrino anomaly and the result of the LSND experiment. These indications and the negative results of numerous short-baseline (SBL) neutrino experiments can be accommodated in the two four-neutrino schemes A and B presented in Eq.(3.1) [25–27].

Working in the framework of the neutrino mixing schemes A and B, we have derived constraints on the parameters $I_{\alpha\beta}$ ($\alpha, \beta = e, \mu, \tau$) (see Eq.(3.14)) that characterize CP violation in $\nu_{\alpha}^{(-)} \rightarrow \nu_{\beta}^{(-)}$ LBL neutrino oscillation experiments in vacuum. These parameters are given in terms of the quantities $I_{\alpha\beta;jk}$ which appear in the general CP-odd asymmetries (see Eqs.(2.13) and (2.14)) as $I_{\alpha\beta} = I_{\alpha\beta;12}$ in scheme A and $I_{\alpha\beta} = I_{\alpha\beta;34}$ in scheme B. We have developed methods for deriving upper bounds on the parameters $I_{\alpha\beta}$ from the data of SBL experiments which can be applied not only to the schemes A and B but to arbitrary schemes with any number of neutrinos. We have shown that the CP-odd parameter $I_{e\mu}$ is bounded by $|I_{e\mu}| \lesssim 10^{-2}$ (see Fig. 2) and a similar suppression applies to $I_{e\tau}$. On the other hand, sizable CP violation can be expected in $\nu_{\mu} \rightarrow \nu_{\tau}$ oscillations. The CP-odd parameter relative to this channel could be close to its maximally allowed value $|I_{\mu\tau}|_{\text{max}} = 2/3\sqrt{3} \approx 0.385$, resulting from the unitarity of the mixing matrix (see Fig. 3).

For LBL accelerator experiments the matter background is important. In this case the parameters $I_{\alpha\beta;jk}$ for neutrinos (antineutrinos) are replaced by the CP-violating parameters $I'_{\alpha\beta;jk}$ ($\bar{I}'_{\alpha\beta;jk}$) which include matter effects (see Eq.(6.7)). Using a physically motivated approximate method of incorporating matter effects [50], we have demonstrated that the quantities $|I'_{\alpha\beta}|$ ($|\bar{I}'_{\alpha\beta}|$) are bounded by the same functions of the SBL mass-squared difference Δm^2 as $|I_{\alpha\beta}|$ apart from terms of order $a_{CC}/\Delta m^2$. Therefore, the bounds depicted in Figs. 2 and 3 apply also to the corresponding $I'_{\alpha\beta}$ and $\bar{I}'_{\alpha\beta}$. However, although finding $I'_{\alpha\beta} \neq 0$ and/or $\bar{I}'_{\alpha\beta} \neq 0$ would prove the existence of CP violation in the neutrino mixing matrix U , the knowledge of the parameters $I'_{\alpha\beta}$ and/or $\bar{I}'_{\alpha\beta}$ cannot easily be transformed into information on $I_{\alpha\beta}$ and thus U , because both sets of parameters are related in complicated, non-linear way involving also the ‘‘matter potentials’’ a_{CC} , a_{NC} and the mass-squared difference relevant for LBL neutrino oscillations.

We have also shown that in matter a second CP-violating parameter $J'_{\alpha\beta}$ (given by $J'_{\alpha\beta} = I'_{\alpha\beta;34}$ in scheme A and $J'_{\alpha\beta} = I'_{\alpha\beta;12}$ in scheme B) appears in the $\nu_\alpha \rightarrow \nu_\beta$ transition probability. Its contribution is only significant if the oscillation phase ω defined in Eq.(6.19) is sufficiently large. An evaluation of the maximal value that the phase ω can assume in accelerator LBL experiments shows that the contribution of $J'_{\alpha\beta}$ could be relevant for baselines longer than ~ 100 km (see Eq.(6.21)). We have argued that the parameter $J'_{\alpha\beta}$ (and the analogous parameter $\bar{J}'_{\alpha\beta}$ for antineutrinos) is subject to the same bounds as $J_{\alpha\beta}$ (with $J_{\alpha\beta} \equiv I_{\alpha\beta;34}$ in scheme A and $J_{\alpha\beta} \equiv I_{\alpha\beta;12}$ in scheme B). These bounds are presented in Eqs.(6.25)–(6.28) and their numerical values obtained from the results of disappearance and appearance SBL neutrino oscillation experiments are shown by the curves in Figs. 4 and 5. There is no analogue of the parameters $J'_{\alpha\beta}$ and $\bar{J}'_{\alpha\beta}$ in the 3-neutrino case.

Since a measurement of the CP-odd asymmetries $D_{\alpha;\beta}$ defined in Eq.(2.8) does not allow to obtain direct information on CP violation if matter effects are important, we have considered the long-baseline T-odd asymmetries $T_{\alpha;\beta}$ ($\bar{T}_{\alpha;\beta}$) defined in Eq.(6.12). Since the matter contribution to the effective neutrino and antineutrino Hamiltonians (6.1), (6.2) is real and the matter density is symmetric along the path of the neutrino beam in terrestrial LBL experiments (to a good approximation it is even constant for baselines shorter than ~ 4000 km) the matter effects are T-symmetric. Therefore, the T-odd asymmetries $T_{\alpha;\beta}$ ($\bar{T}_{\alpha;\beta}$) are only different from zero if CP is violated in the lepton mixing matrix U . We have shown that in the four-neutrino schemes A and B the T-odd asymmetries depend on the parameters $I'_{\alpha\beta}$ ($\bar{I}'_{\alpha\beta}$) and $J'_{\alpha\beta}$ ($\bar{J}'_{\alpha\beta}$) (see Eq.(6.20)). Hence, they are subject to the constraints derived from the results of SBL experiments.

In conclusion, we have shown that in the four-neutrino schemes A and B the channels $\nu_\mu \overset{(-)}{\rightleftharpoons} \nu_e$ are disfavoured for the search of CP-violation effects in future LBL oscillation experiments, the channels $\nu_e \overset{(-)}{\rightleftharpoons} \nu_\tau$ could allow to reveal relatively large CP-violating effects where matter plays an important role and the channels $\nu_\mu \overset{(-)}{\rightleftharpoons} \nu_\tau$ could show CP-violating effects as large as is allowed by the unitarity of the neutrino mixing matrix.

APPENDIX A: DERIVATION OF THE AMPLITUDE BOUND

In this appendix we discuss the derivation of the ‘‘amplitude bound’’. The starting point is the quantity

$$I_{\alpha\beta} = 4 \operatorname{Im} [U_{\alpha 1} U_{\beta 1}^* U_{\alpha 2}^* U_{\beta 2}] \quad (\alpha \neq \beta), \quad (\text{A1})$$

which determines the CP-odd asymmetry in the four-neutrino scheme A. The same bound can be derived in the scheme B with the change of indices (3.8).

It is obvious that $I_{\alpha\beta}$ is invariant under the phase transformations

$$U_{\alpha j} \rightarrow e^{i\gamma_j} U_{\alpha j}, \quad U_{\beta j} \rightarrow e^{i\gamma_j} U_{\beta j}, \quad (\text{A2})$$

where the γ_j are arbitrary phases. Thus the elements $U_{\alpha j}$ can be taken to be real. Taking into account the definition (3.2), we can write

$$U_{\alpha j} = \sqrt{c_\alpha} e_j^{(1)} \quad \text{with } j = 1, 2 \quad (\text{A3})$$

and the orthonormal basis

$$e^{(1)}(\theta) = (\cos \theta, \sin \theta), \quad e^{(2)}(\theta) = (-\sin \theta, \cos \theta). \quad (\text{A4})$$

We expand $U_{\beta j}$ with respect to this basis as

$$U_{\beta j} = \sqrt{c_\beta} \sum_{\rho=1,2} p_\rho e_j^{(\rho)}, \quad (\text{A5})$$

where p_1 and p_2 are complex coefficients such that

$$\sum_{\rho=1,2} |p_\rho|^2 = 1. \quad (\text{A6})$$

With the help of Eqs.(A3)–(A6) we easily find

$$I_{\alpha\beta} = 2 c_\alpha c_\beta \sin 2\theta \operatorname{Im}(p_1^* p_2) = 2 c_\alpha c_\beta |p_1| \sqrt{1 - |p_1|^2} \sin 2\theta \sin \delta, \quad (\text{A7})$$

where δ is the phase of $p_1^* p_2$.

The parameter $|p_1|$ is connected to the oscillation amplitude $A_{\alpha;\beta}$ and the parameters c_α, c_β . In fact, from Eqs.(A3) and (A5) we have

$$A_{\alpha;\beta} = 4 \left| \sum_{j=1,2} U_{\alpha j} U_{\beta j}^* \right|^2 = 4 c_\alpha c_\beta |p_1|^2, \quad (\text{A8})$$

which implies $|p_1| = \sqrt{A_{\alpha;\beta}/4c_\alpha c_\beta}$. Inserting this expression in Eq.(A7), we obtain

$$I_{\alpha\beta} = \frac{1}{2} \sqrt{A_{\alpha;\beta} (4 c_\alpha c_\beta - A_{\alpha;\beta})} \sin 2\theta \sin \delta \quad (\text{A9})$$

and thus we arrive at the ‘‘amplitude bound’’

$$|I_{\alpha\beta}| \leq \frac{1}{2} \sqrt{A_{\alpha;\beta} (4 c_\alpha c_\beta - A_{\alpha;\beta})}. \quad (\text{A10})$$

Let us stress that this derivation is based only on the obvious inequality

$$|\sin 2\theta \sin \delta| \leq 1. \quad (\text{A11})$$

Since c_α, c_β and $A_{\alpha;\beta}$ do not restrict θ and δ , the bound (A10) is the optimal one.

APPENDIX B: DERIVATION OF THE UNITARITY BOUND

Up to now we did not use the unitarity of the mixing matrix. Taking this fact into account will allow us to obtain an upper bound on $|I_{\alpha\beta}|$ depending solely on c_α and c_β .

The unitarity of the mixing matrix tells us that

$$\sum_{j=1,2} U_{\alpha j} U_{\beta j}^* = - \sum_{j=3,4} U_{\alpha j} U_{\beta j}^*. \quad (\text{B1})$$

This relation allows to write the oscillation amplitude $A_{\alpha;\beta}$ in the two forms of Eq.(3.7). Using the Cauchy–Schwarz inequality, one can see that (in the scheme A)

$$A_{\alpha;\beta} = 4 \left| \sum_{j=3,4} U_{\alpha j} U_{\beta j}^* \right|^2 \leq 4 \left(\sum_{j=3,4} |U_{\alpha j}|^2 \right) \left(\sum_{j=3,4} |U_{\beta j}|^2 \right) = 4 (1 - c_\alpha) (1 - c_\beta). \quad (\text{B2})$$

The right-hand side of the inequality (A10), as a function of $A_{\alpha;\beta}$, reaches its maximum, $c_\alpha c_\beta$, at (here we do not take into account possible experimental information on $A_{\alpha;\beta}$)

$$(A_{\alpha;\beta})_0 = 2 c_\alpha c_\beta. \quad (\text{B3})$$

Consequently, if the condition

$$2 (1 - c_\alpha) (1 - c_\beta) \geq c_\alpha c_\beta \quad (\text{B4})$$

is satisfied, the upper bound (B2) on $A_{\alpha;\beta}$ is larger than $(A_{\alpha;\beta})_0$. In this case we have

$$|I_{\alpha\beta}| \leq c_\alpha c_\beta. \quad (\text{B5})$$

If the condition (B4) is not fulfilled, the upper bound (B2) is smaller than $(A_{\alpha;\beta})_0$ and has to be inserted for $A_{\alpha;\beta}$ into Eq.(A10), leading to

$$|I_{\alpha\beta}| \leq 2 \sqrt{(c_\alpha + c_\beta - 1) (1 - c_\alpha) (1 - c_\beta)}. \quad (\text{B6})$$

Thus, we arrive at the “unitarity bound”

$$|I_{\alpha\beta}| \leq f(c_\alpha, c_\beta), \quad (\text{B7})$$

with the function

$$f(x, y) = \begin{cases} f_1 \equiv xy & \text{for } 2(1-x)(1-y) \geq xy, \\ f_2 \equiv 2[(x+y-1)(1-x)(1-y)]^{1/2} & \text{for } 2(1-x)(1-y) < xy, \end{cases} \quad (\text{B8})$$

defined on the unit square $0 \leq x \leq 1, 0 \leq y \leq 1$. The function

$$g(x) = \frac{2(1-x)}{2-x} \quad (\text{B9})$$

represents the borderline separating the two regions in the definition of the function (B8). It is clear from our derivation (and also easy to check) that f is continuous along this borderline.

APPENDIX C: DISCUSSION OF THE FUNCTION f

Since we do not have definite experimental values of c_α and c_β , but only bounds on these quantities (see Eqs.(3.3) and (3.4)), which define allowed rectangles in the square $0 \leq c_\alpha \leq 1$, $0 \leq c_\beta \leq 1$, we are interested in the behaviour of f in order to evaluate the unitarity bound.

From the partial derivative of f in the region $y \geq g(x)$,

$$\frac{\partial f}{\partial x} = \frac{\partial f_2}{\partial x} \propto (2 - 2x - y), \tag{C1}$$

one can see that, at fixed y , the function f increases monotonously from $x = 0$ to the point $x = 1 - y/2$, where the partial derivative in Eq.(C1) is zero. The points $x = 1 - y/2$ lie on the straight line $y_1(x) = 2 - 2x$. In the range $1 - y/2 \leq x \leq 1$ the function f decreases monotonously. Taking into account the symmetry $f(x, y) = f(y, x)$, we see that at fixed x the function f increases monotonously from $y = 0$ to the point $y = 1 - x/2$, where the partial derivative of f with respect to y is zero. These points lie on the straight line $y_2(x) = 1 - x/2$. Beyond this line f decreases monotonously. Note that both straight lines lie in the range of f_2 .

Figure 1 shows a contour plot of the function $f(x, y)$, together with the lines y_1 and y_2 which intersect at the point

$$x = y = \frac{2}{3}. \tag{C2}$$

At this point both partial derivatives of f are equal to zero and therefore the point (C2) corresponds to the absolute maximum of f , given by

$$f_{\max} = f_2\left(\frac{2}{3}, \frac{2}{3}\right) = \frac{2}{3^{3/2}} \approx 0.385. \tag{C3}$$

This number constitutes the absolute upper bound for $|I_{\alpha\beta}|$.

REFERENCES

- [1] J.H. Christenson, J.W. Cronin, V.L. Fitch and R. Turlay, *Phys. Rev. Lett.* **13**, 138 (1964).
- [2] W. Bernreuther, *CP Violation in Weak Decays and Elsewhere*, talk given at the *20th Johns Hopkins Workshop*, Heidelberg, June 1996, preprint hep-ph/9701357; Andrzej J. Buras, *CKM Matrix: Present and Future*, talk given at the *Symposium on Heavy Flavours*, Santa Barbara, July 7-July 11, 1997, preprint hep-ph/9711217.
- [3] M. Kobayashi and T. Maskawa, *Prog. Theor. Phys.* **49**, 652 (1973).
- [4] B.T. Cleveland *et al.*, *Nucl. Phys. B (Proc. Suppl.)* **38**, 47 (1995).
- [5] K.S. Hirata *et al.*, *Phys. Rev. D* **44**, 2241 (1991).
- [6] GALLEX Coll., W. Hampel *et al.*, *Phys. Lett. B* **388**, 384 (1996).
- [7] J.N. Abdurashitov *et al.*, *Phys. Rev. Lett.* **77**, 4708 (1996).
- [8] K. Inoue, Talk presented at *TAUP97*, September 7-11, 1997, Laboratori Nazionali del Gran Sasso, Assergi (Italy).
- [9] Y. Fukuda *et al.*, *Phys. Lett. B* **335**, 237 (1994).
- [10] R. Becker-Szendy *et al.*, *Nucl. Phys. B (Proc. Suppl.)* **38**, 331 (1995).
- [11] W.W.M. Allison *et al.*, *Phys. Lett. B* **391**, 491 (1997).
- [12] K. Martens, Talk presented at the *International Europhysics Conference on High Energy Physics*, 19–26 August 1997, Jerusalem, Israel (<http://www.cern.ch/hep97/abstract/-tpa10.htm>); E. Kearns, Talk presented at the Conference on *Solar Neutrinos: News About SNU's*, 2–6 December 1997, Santa Barbara, California (<http://doug-pc.itp.ucsb.edu/online/snu/>).
- [13] C. Athanassopoulos *et al.*, *Phys. Rev. Lett.* **77**, 3082 (1996).
- [14] GALLEX Coll., P. Anselmann *et al.*, *Phys. Lett. B* **285**, 390 (1992); P.I. Krastev and S.T. Petcov, *ibid.* **299**, 99 (1993); N. Hata and P.G. Langacker, *Phys. Rev. D* **50**, 632 (1994); G. Fiorentini *et al.*, *ibid.* **49**, 6298 (1994).
- [15] V. Barger, R.J.N. Phillips and K. Whisnant, *Phys. Rev. Lett.* **69**, 3135 (1992); P.I. Krastev and S.T. Petcov, *Phys. Rev. Lett.* **72**, 1960 (1994).
- [16] S.P. Mikheyev and A.Yu. Smirnov, *Yad. Fiz.* **42**, 1441 (1985) [*Sov. J. Nucl. Phys.* **42**, 913 (1985)]; *Il Nuovo Cimento C* **9**, 17 (1986); L. Wolfenstein, *Phys. Rev. D* **17**, 2369 (1978); *ibid.* **20**, 2634 (1979).
- [17] S.M. Bilenky and B. Pontecorvo, *Phys. Rep.* **41**, 225 (1978).
- [18] S.M. Bilenky and S.T. Petcov, *Rev. Mod. Phys.* **59**, 671 (1987).
- [19] C.W. Kim and A. Pevsner, *Neutrinos in Physics and Astrophysics*, Contemporary Concepts in Physics, Vol. 8, (Harwood Academic Press, Chur, Switzerland, 1993).
- [20] V. Barger *et al.*, *Phys. Rev. D* **22**, 1636 (1980); S.M. Bilenky and F. Niedermayer, *Yad. Fiz.* **34**, 1091 (1981) [*Sov. J. Nucl. Phys.* **34**, 606 (1981)].
- [21] Y. Suzuki, Proc. of *Neutrino 96*, Helsinki, June 1996, edited by K. Enqvist *et al.*, p. 237 (World Scientific, Singapore, 1997).
- [22] MINOS Coll., D. Ayres *et al.*, NUMI-L-63, February 1995.
- [23] ICARUS Coll., P. Cennini *et al.*, LNGS-94/99-I, May 1994.
- [24] NOE Coll., G.C. Barbarino *et al.*, INFN/AE-96/11, May 1996; AQUA-RICH Coll., T. Ypsilantis *et al.*, LPC/96-01, CERN-LAA/96-13; OPERA Coll., H. Shibuya *et al.*, CERN-SPSC-97-24.

- [25] S.M. Bilenky, C. Giunti and W. Grimus, Proc. of *Neutrino 96*, Helsinki, June 1996, edited by K. Enqvist et. al., p. 174 (World Scientific, Singapore, 1997).
- [26] S.M. Bilenky, C. Giunti and W. Grimus, preprint hep-ph/9607372, to appear in *Z. Phys. C*.
- [27] N. Okada and O. Yasuda, *Int. J. Mod. Phys. A* **12**, 3669 (1997).
- [28] M. Tanimoto, *Phys. Rev. D* **55**, 322 (1997).
- [29] J. Arafune and J. Sato, *Phys. Rev. D* **55**, 1653 (1997); J. Arafune, M. Koike and J. Sato, *Phys. Rev. D* **56**, 3093 (1997).
- [30] H. Minakata and H. Nunokawa, preprint TMUP-HEL-9704 (hep-ph/9705208); preprint TMUP-HEL-9705 (hep-ph/9706281).
- [31] T.K. Kuo and J. Pantaleone, *Phys. Lett. B* **198**, 406 (1995).
- [32] S. Geer, preprint Fermilab-PUB-97/389 (hep-ph/9712290).
- [33] R.N. Mohapatra, Talk presented at the *Workshop on Physics with the First Muon Collider*, Fermilab, 6–9 November 1997, preprint hep-ph/9711444.
- [34] M. Doi *et al.*, *Phys. Lett. B* **102**, 323 (1981); L. Wolfenstein, *Phys. Lett. B* **107**, 77 (1981); S.M. Bilenky *et al.*, *Nucl. Phys. B* **247**, 61 (1984); B. Kayser, *Phys. Rev. D* **30**, 1023 (1984).
- [35] S.M. Bilenky, J. Hosek and S.T. Petcov, *Phys. Lett. B* **94**, 495 (1980); M. Doi *et al.*, *Phys. Lett. B* **102**, 323 (1981).
- [36] C. Jarlskog, *Phys. Rev. Lett.* **55**, 1039 (1985); *Z. Phys. C* **29**, 491 (1985); C. Jarlskog and R. Stora, *Phys. Lett. B* **208**, 268 (1988); C. Jarlskog, Proc. of *CP Violation*, Ed. C. Jarlskog, Advanced Series in High Energy Physics Vol. 3 (World Scientific, Singapore, 1989), p. 3.
- [37] D.D. Wu, *Phys. Rev. D* **33**, 860 (1986); I. Dunietz, O.W. Greenberg and D.D. Wu, *Phys. Rev. Lett.* **55**, 2935 (1985).
- [38] J.D. Bjorken and I. Dunietz, *Phys. Rev. D* **36**, 2109 (1987); I. Dunietz, *Ann. Phys.* **184**, 350 (1988).
- [39] J.T. Peltoniemi and J.W.F. Valle, *Nucl. Phys. B* **406**, 409 (1993); D.O. Caldwell and R.N. Mohapatra, *Phys. Rev. D* **48**, 3259 (1993); Z. Berezhiani and R.N. Mohapatra, *Phys. Rev. D* **52**, 6607 (1995); J.R. Primack *et al.*, *Phys. Rev. Lett.* **74**, 2160 (1995); E. Ma and P. Roy, *Phys. Rev. D* **52**, R4780 (1995); R. Foot and R.R. Volkas, *Phys. Rev. D* **52**, 6595 (1995); E.J. Chun *et al.*, *Phys. Lett. B* **357**, 608 (1995); J.J. Gomez-Cadenas and M.C. Gonzalez-Garcia, *Z. Phys. C* **71**, 443 (1996); S. Goswami, *Phys. Rev. D* **55**, 2931 (1997); A.Yu. Smirnov and M. Tanimoto, *Phys. Rev. D* **55**, 1665 (1997); E. Ma, *Mod. Phys. Lett. A* **11**, 1893 (1996).
- [40] S.M. Bilenky, C. Giunti, C.W. Kim and S.T. Petcov, *Phys. Rev. D* **54**, 4432 (1996).
- [41] B. Achkar *et al.*, *Nucl. Phys. B* **434**, 503 (1995).
- [42] F. Dydak *et al.*, *Phys. Lett. B* **134**, 281 (1984).
- [43] I.E. Stockdale *et al.*, *Phys. Rev. Lett.* **52**, 1384 (1984).
- [44] S.M. Bilenky, A. Bottino, C. Giunti and C.W. Kim, *Phys. Rev. D* **54**, 1881 (1996).
- [45] L.A. Ahrens *et al.*, *Phys. Rev. D* **36**, 702 (1987).
- [46] L. Borodovsky *et al.*, *Phys. Rev. Lett.* **68**, 274 (1992).
- [47] A. Romosan *et al.*, *Phys. Rev. Lett.* **78**, 2912 (1997).
- [48] N. Ushida, *Phys. Rev. Lett.* **57**, 2897 (1986).
- [49] K.S. McFarland *et al.*, *Phys. Rev. Lett.* **75**, 3993 (1995).

- [50] S.M. Bilenky, C. Giunti and W. Grimus, preprint hep-ph/9710209, Phys. Rev. D **57** (1998) in press.
- [51] S.M. Bilenky, A. Bottino, C. Giunti and C.W. Kim, Phys. Lett. B **356**, 273 (1995).
- [52] M. Apollonio *et al.*, preprint hep-ex/9711002.

FIGURES

FIG.1. Contour plot of the function $f(x, y)$ given in Eq.(4.2). The dotted line is the borderline $g(x) = 2(1 - x)/(2 - x)$ between the regions where $f = f_1$ and $f = f_2$. The two solid lines represent the functions $y_1(x) = 2 - 2x$ and $y_2(x) = 1 - x/2$.

FIG.2. Upper bound for the parameter $|I_{e\mu}|$ which characterizes the CP-odd asymmetry in the $\nu_\mu \rightarrow \nu_e$ channel for the SBL parameter Δm^2 in the range $10^{-1} \text{ eV}^2 \leq \Delta m^2 \leq 10^3 \text{ eV}^2$. The solid curve represents the upper function in Eq.(4.4) and is obtained from the 90% CL exclusion plot of the Bugey $\bar{\nu}_e \rightarrow \bar{\nu}_e$ experiment. The dash-dotted curve improves the solid curve where $a_\mu^0 \leq a_e^0/2$ (the lower function in Eq.(4.4)). It is obtained from the 90% CL exclusion plots of the Bugey $\bar{\nu}_e \rightarrow \bar{\nu}_e$ experiment and the CDHS and CCFR $\nu_\mu \rightarrow \nu_\mu$ experiments. The dashed curve is obtained from the 90% CL exclusion plots of the Bugey $\bar{\nu}_e \rightarrow \bar{\nu}_e$ experiment and the BNL E734, BNL E776 and CCFR $\nu_\mu \rightarrow \nu_e$ and $\bar{\nu}_\mu \rightarrow \bar{\nu}_e$ experiments (see the upper function in Eq.(4.8)). The shadowed region corresponds to the range (1.3) of Δm^2 allowed at 90% CL by the results of the LSND experiment. The solid curve represents also an upper bound for $|I_{e\tau}|$.

FIG.3. Upper bound for the parameter $|I_{\mu\tau}|$ which characterizes the CP-odd asymmetry in the $\nu_\mu \rightarrow \nu_\tau$ channel. The solid curve is obtained from the 90% CL exclusion plots of the CDHS and CCFR $\nu_\mu \rightarrow \nu_\mu$ experiments (see Eq.(4.5)). The dashed curve is obtained from the 90% CL exclusion plots of the FNAL E531 and CCFR $\nu_\mu \rightarrow \nu_\tau$ experiments (see Eq.(4.9)). The shadowed region corresponds to the range (1.3) of Δm^2 allowed at 90% CL by the results of the LSND experiment.

FIG.4. Upper bound for the parameter $|J_{e\mu}|$ (see Eq.(6.22)). The solid curve represents the unitarity bound (6.25) and is obtained from the 90% CL exclusion plots of the Bugey $\bar{\nu}_e \rightarrow \bar{\nu}_e$ experiment and those of the CDHS and CCFR $\nu_\mu \rightarrow \nu_\mu$ experiments. The dashed curve represents the value of the amplitude bound (6.26) obtained from the 90% CL exclusion plots of the CDHS and CCFR $\nu_\mu \rightarrow \nu_\mu$ experiments and those of the BNL E734, BNL E776 and CCFR $\nu_\mu \rightarrow \nu_e$ and $\bar{\nu}_\mu \rightarrow \bar{\nu}_e$ experiments. The shadowed region corresponds to the range (1.3) of Δm^2 allowed at 90% CL by the results of the LSND experiment.

FIG.5. Upper bound for the parameter $|J_{\mu\tau}|$ (see Eq.(6.22)). The solid curve represents the unitarity bound (6.27) obtained from the 90% CL exclusion plots of the CDHS and CCFR $\nu_\mu \rightarrow \nu_\mu$ experiments. The dashed curve depicts the value of the amplitude bound (6.28) obtained from the 90% CL exclusion plots of the CDHS and CCFR $\nu_\mu \rightarrow \nu_\mu$ experiments and those of the FNAL E531 and CCFR $\nu_\mu \rightarrow \nu_\tau$ experiments. The shadowed region corresponds to the range (1.3) of Δm^2 allowed at 90% CL by the results of the LSND experiment.

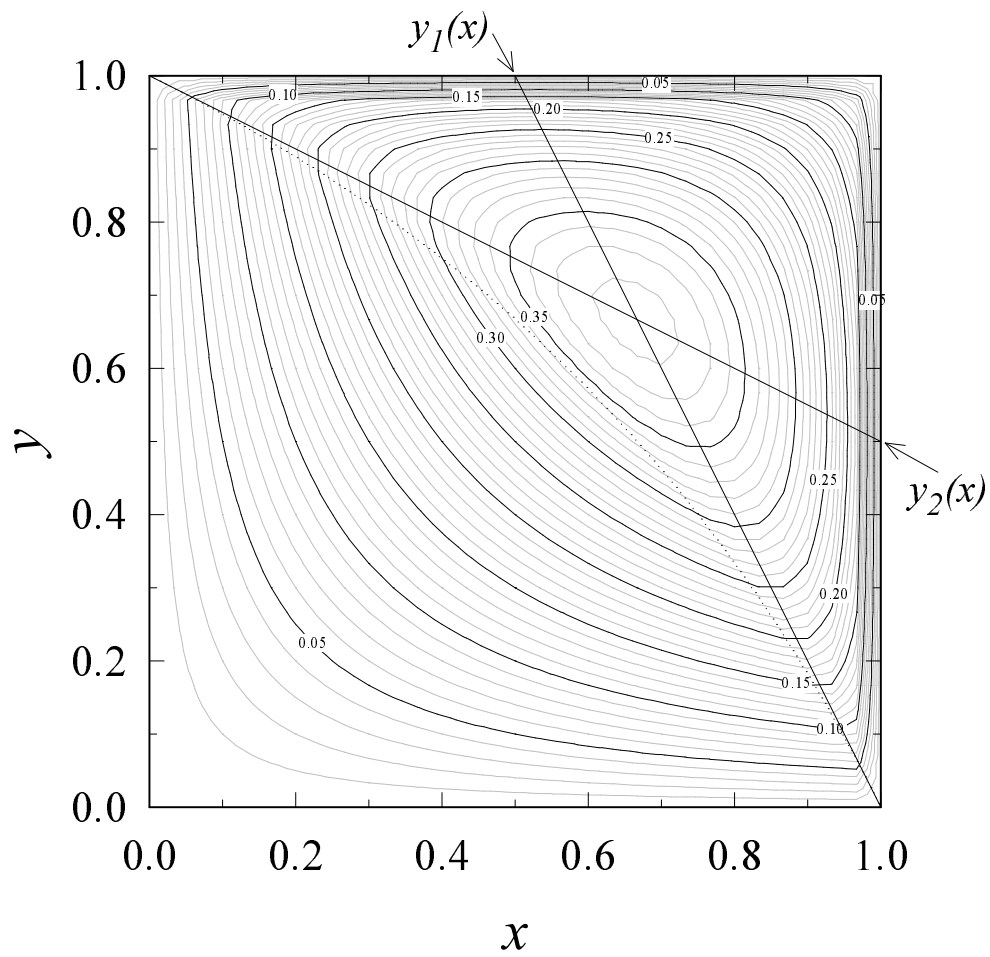


Figure 1

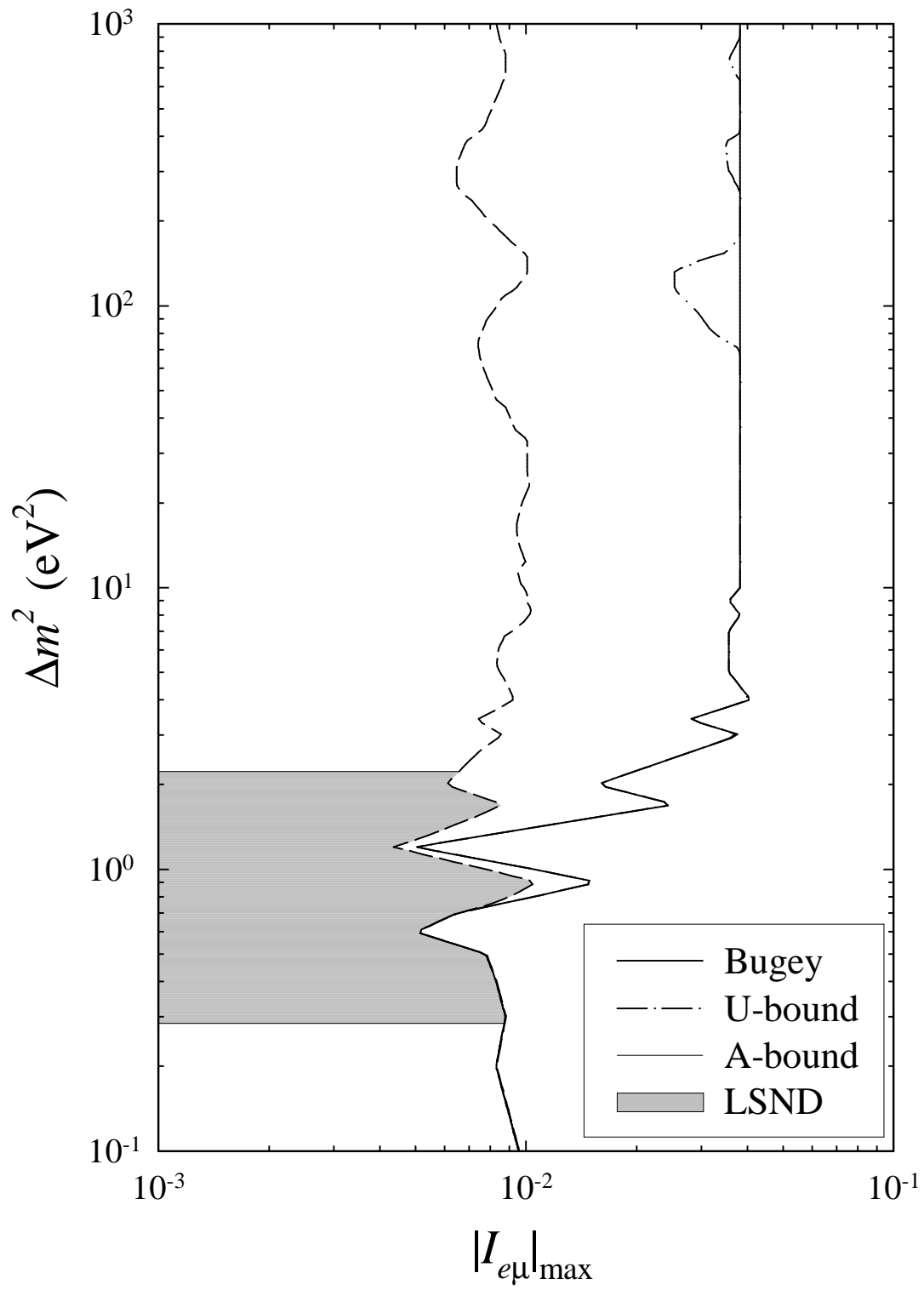


Figure 2

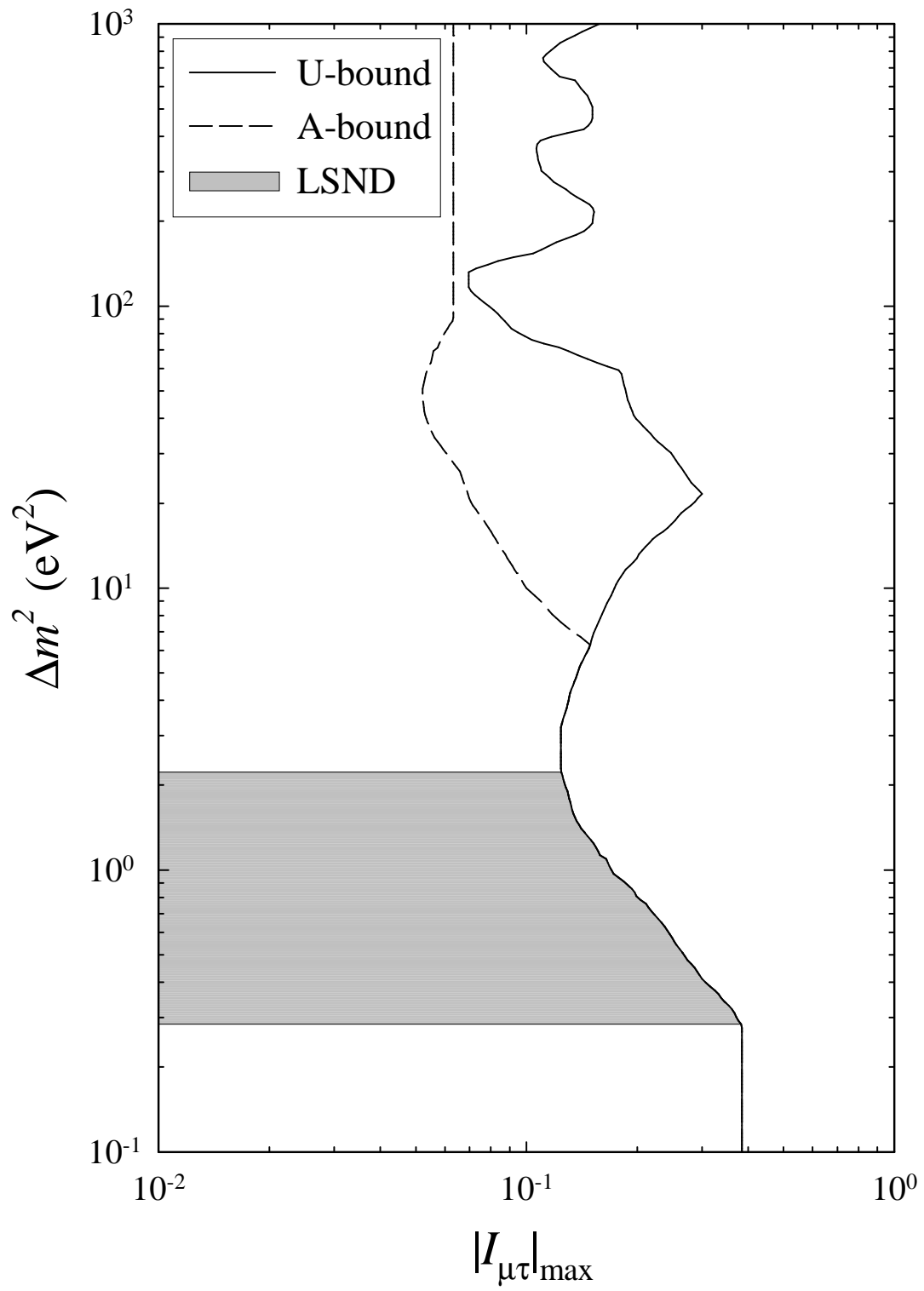


Figure 3

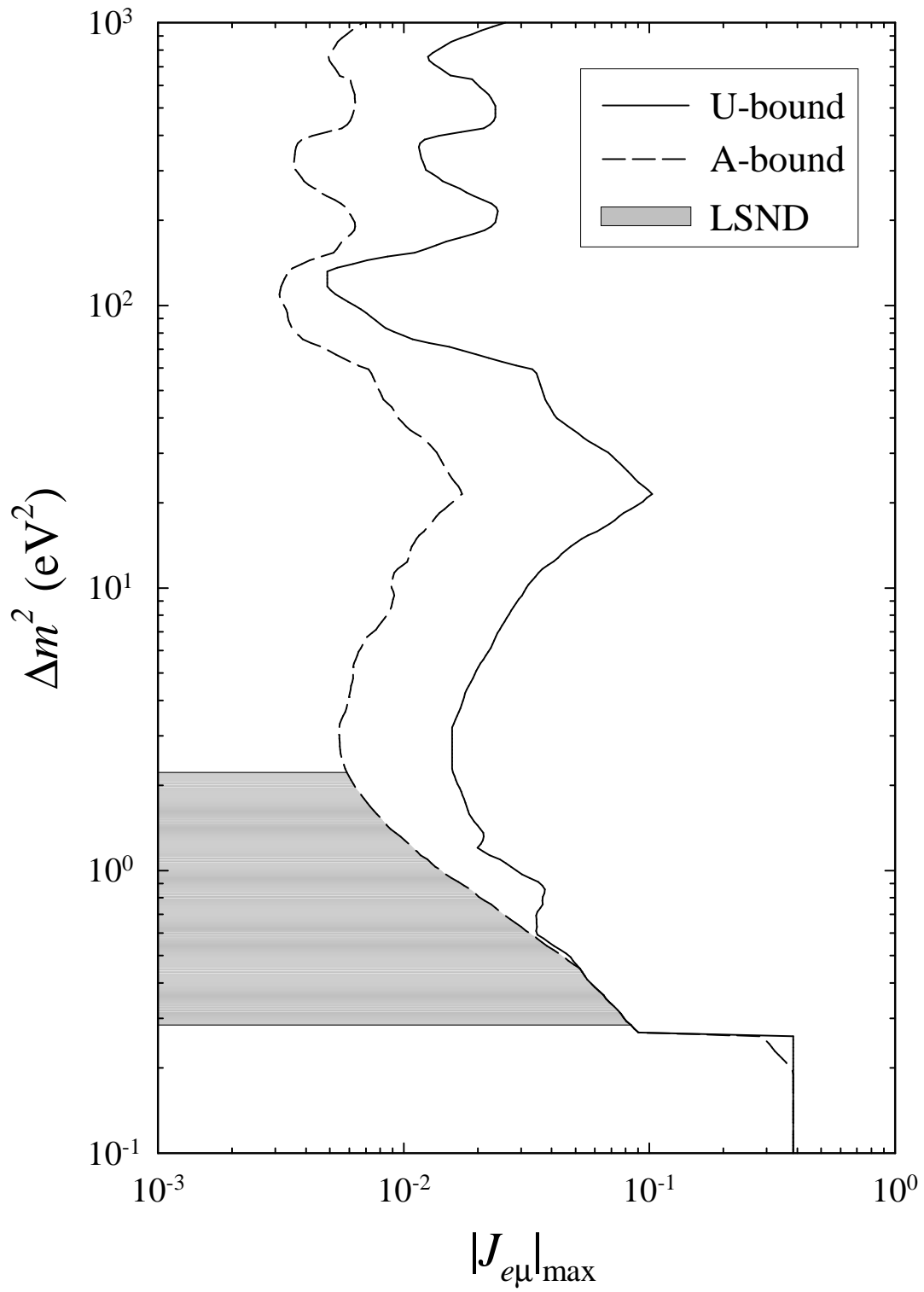


Figure 4

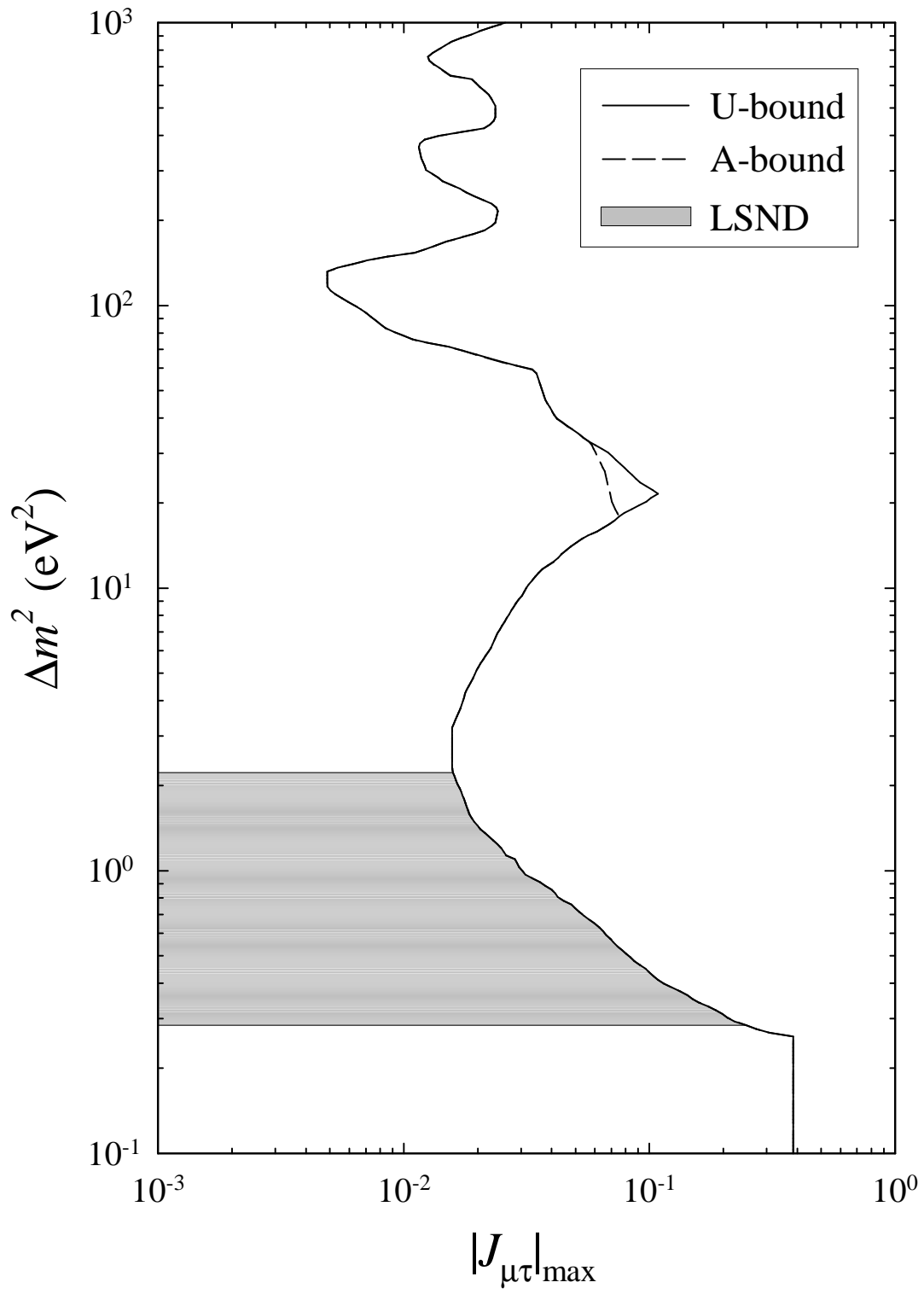


Figure 5